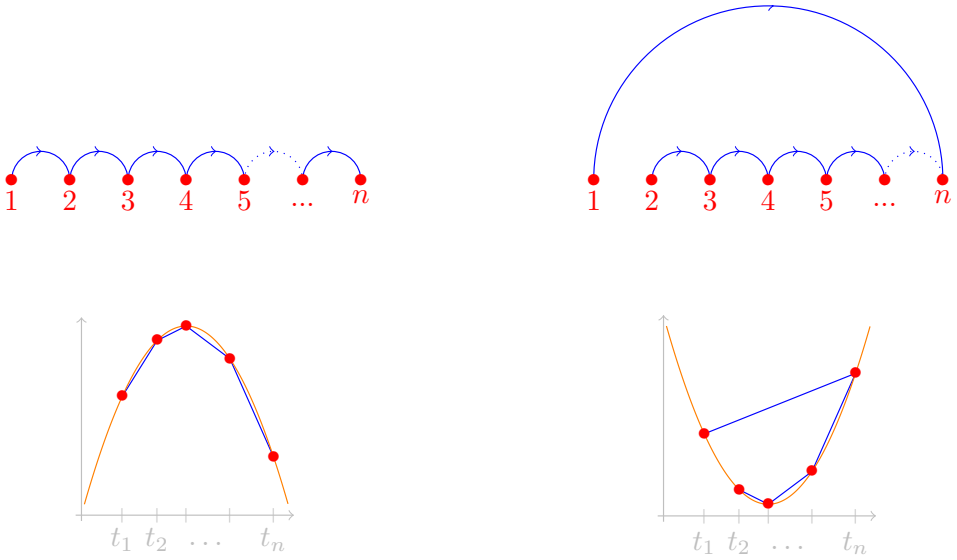

Figure 44: The two arborescences $A_m^{(2)}$ (Left) and $A_M^{(2)}$ (Right) appearing as vertices of $\Pi(\mathsf{Cyc}_2(\boldsymbol{t}), \boldsymbol{e}_1)$ for all $\boldsymbol{t} \in \mathsf{O}_n^\circ$, and degree 2 polynomials capturing them.

Proof. As $\mathsf{Cyc}_3(\boldsymbol{t})$ is a simplicial 3-dimensional polytope, its facets are triangles. By Gale's evenness condition (see [Zie98] Theorem 0.7), the vertices $\boldsymbol{\gamma}_d(t_a)$, $\boldsymbol{\gamma}_d(t_b)$ and $\boldsymbol{\gamma}_d(t_c)$ form a facet when there is an even number of elements from $\{a, b, c\}$ between the elements of $[n]\backslash\{a, b, c\}$. This means either $\{a, b, c\} = \{1, i, i+1\}$ for some $1 < i < n$, or $\{a, b, c\} = \{i, i+1, n\}$ for some $1 < i < n$. Thus, edges of $\mathsf{Cyc}_3(\boldsymbol{t})$ are $[\boldsymbol{\gamma}_d(t_i), \boldsymbol{\gamma}_d(t_{i+1})]$, $[\boldsymbol{\gamma}_d(t_1), \boldsymbol{\gamma}_d(t_i)]$ and $[\boldsymbol{\gamma}_d(t_i), \boldsymbol{\gamma}_d(t_n)]$. Orienting them along $\boldsymbol{e}_1$ yields the lemma. □

Definition 3.42. A *3-arborescence* is a map $A : [n] \to [n]$ with $A(i) \in \{i+1, n\}$ for $i \neq 1$ (and $A(1) \in [n]$).

Hence, by Lemma 3.41, each vertex of $\Pi(\mathsf{Cyc}_3(\boldsymbol{t}), \boldsymbol{e}_1)$ can be associated to a 3-arborescence. Note that such arborescences can have crossings, contrarily to what we discussed so far.

The fact that $\mathsf{Cyc}_3(\boldsymbol{t})$ is not neighborly also modifies the notion of capturing an arborescence.

Proposition 3.43. *A 3-arborescence A corresponds to a vertex of $\Pi(\mathsf{Cyc}_3(\boldsymbol{t}), \boldsymbol{e}_1)$ if and only if there exists a polynomial P of degree at most 3 such that (denoting $\tau(a, b) = \frac{P(b)-P(a)}{b-a}$ as usual):*

- *for all $j \notin \{1, A(1)\}$, $\tau(1, A(1)) > \tau(1, j)$.*
- *for all $i \neq 1$, if $A(i) = i+1$, then $\tau(i, i+1) > \tau(i, n)$, else if $A(i) = n$, then $\tau(i, n) > \tau(i, i+1)$.*

Proof. Fix $\boldsymbol{t} = (t_1, ..., t_n)$. A 3-arborescence A corresponds to a max-slope arborescence for the linear program $(\mathsf{Cyc}_3(\boldsymbol{t}), \boldsymbol{e}_1)$ if there exists $\boldsymbol{w} = (w_1, w_2, w_3) \in \mathbb{R}^3$ such that $A(i) = A^{\boldsymbol{w}}(\boldsymbol{\gamma}_d(t_i))$ for all $i \in [n]$, with $A^{\boldsymbol{w}}(\boldsymbol{v}) = \operatorname{argmax}\left\{ \frac{\langle \boldsymbol{w}, \boldsymbol{u}-\boldsymbol{v} \rangle}{\langle \boldsymbol{e}_1, \boldsymbol{u}-\boldsymbol{v} \rangle} : u \ \boldsymbol{e}_1\text{-improving neighbor of } v \right\}$. Denoting by P the univariate polynomial $P(t) = w_3 t^3 + w_2 t^2 + w_1 t$, then $\langle \boldsymbol{\gamma}_d(t_i), \boldsymbol{w} \rangle = P(t_i)$, and the conditions of the proposition precisely describe $A^{\boldsymbol{w}}$. □

Corollary 3.44. *For all $\boldsymbol{t} \in \mathsf{O}_n^\circ$, a 3-arborescence corresponding to one of the vertices of $\Pi(\mathsf{Cyc}_3(\boldsymbol{t}), \boldsymbol{e}_1)$ can have one of the following forms:*

(i) *For $k \in [n-1]$, define $A_k^{(3)}$ by $A_k^{(3)}(i) = i+1$ for $1 \leq i < k$ and $A(i) = n$ for $k \leq i < n$, see Figure 45. There are $n-1$ such arborescences.*

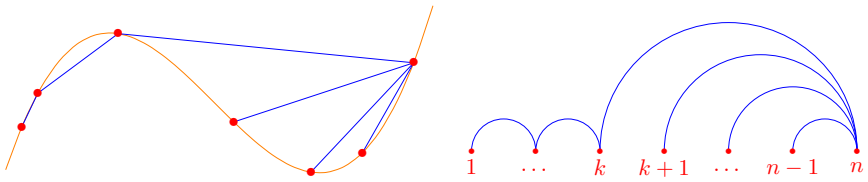

Figure 45: 3-arborescences captured by a degree 3 polynomial with **positive** leading coefficient.

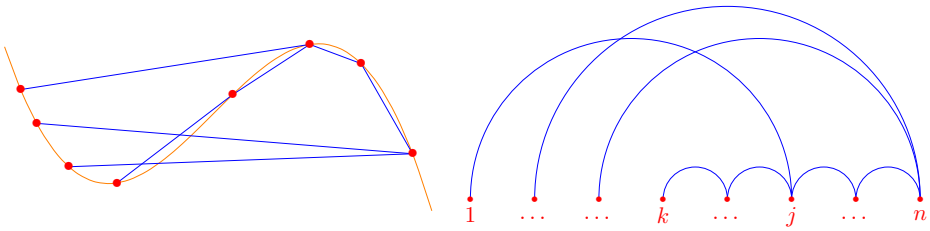

Figure 46: 3-arborescences captured by a degree 3 polynomial with **negative** leading coefficient.

(ii) *For* $1 < k \leq j-1 \leq n-1$ *and* $(j,k) \neq (n,-1)$, *define* $A^{(3)}_{j,k}$ *by* $A^{(3)}_{j,k}(1) = j$, $A^{(3)}_{j,k}(i) = n$ *for* $1 \leq i < k$ *and* $A^{(3)}_{j,k}(i) = i+1$ *for* $k \leq i < n$, *see Figure 46. There are* $\sum_{j=3}^{n}(j-2) - 1 = \binom{n-1}{2} - 1$ *such arborescences.*

Proof. Fix $\boldsymbol{t} \in \mathsf{O}_n^\circ$. Write $P(t) = w_3t^3 + w_2t^2 + w_1t$. If $w_3 = 0$, then P is of degree 2: it can capture A_1 (when $w_2 > 0$) or A_{n-1} (when $w_2 < 0$). There remain two cases.

First, suppose that the leading coefficient of P is positive, *i.e.* $w_3 > 0$. We are going to prove that a 3-arborescence captured by P is necessarily of the form $A^{(3)}_k$ for some $k \in [n-1]$. Indeed, let A be the arborescence captured by P on $\boldsymbol{t}$. By Lemma 3.41, we know that A is a 3-arborescence. Suppose that there exists $i \neq 1$ such that $A(i) = n$ and $A(i+1) = i+2$. Then $\tau(i,n) > \tau(i,i+1)$ and $\tau(i+1,i+2) > \tau(i+1,n)$. By Lemma 3.5, the first inequality gives $\tau(i+1,n) > \tau(i,i+1)$ and the second $\tau(i+2,n) > \tau(i+1,i+2)$. Then $\tau(i+1,i+2) > \tau(i,i+1)$. Thus, as in the proof of Theorem 3.11, there is $\alpha \in]\theta_i, \theta_{i+2}[$ with $P''(\alpha) > 0$ and $\beta \in]\theta_{i+1}, \theta_n[$ with $P''(\beta) < 0$, where $\theta_i < \theta_{i+1} < \theta_n$. But this means that $\alpha < \beta$, which contradicts the fact that the leading coefficient of P is positive.

Consequently, if $A(i) = i+1$, then $A(i') = i'+1$ for all $i' \geq i$. If $A(1) \neq 2$, then the same reasoning applies (with $i = 1$). This proves that $A = A^{(3)}_k$ for some k.

On the other side, if the leading coefficient of P is negative, *i.e.* $w_3 < 0$, then similar arguments apply to prove that, in the 3-arborescence A captured, if $A(i) = i+1$, then $A(i') = i'+1$ for all $i' \geq i$. Suppose that $A(1) = j$ for some $j \in [2,n]$, then $A(j-1) = j$, because, with Lemma 3.5, $\tau(1,j) > \tau(j,n)$, and $\tau(1,j) < \tau(j-1,j)$, thus $\tau(j-1,j) > \tau(j,n)$. This proves that $A = A^{(3)}_{j,k}$ for some $1 < k \leq j-1 \leq n-1$.

As $A_{n-1} = B_{n,n-1}$, we avoid double counting by requiring $(j,k) \neq (n,n-1)$. □

We now want to mimic Theorem 3.16.

Theorem 3.45. *For* $k \in [n-1]$, *we define:*

$$\begin{aligned} \mathsf{P}_3^f\left(A^{(3)}_k, \boldsymbol{t}\right) &= [t_1+t_2+t_3, \quad t_{k-1}+t_k+t_n] \\ \mathsf{P}_3^b\left(A^{(3)}_k, \boldsymbol{t}\right) &= [t_k+t_{k+1}+t_n, \quad t_{n-2}+t_{n-1}+t_n] \end{aligned}$$

For $1 < k \leq j-1 \leq n-1$, we define:

$$\begin{array}{rcl} \mathsf{P}_3^f\left(A_{j,k}^{(3)}, \boldsymbol{t}\right) & = & [\min(t_1+t_j+t_{j+1},\ t_k+t_{k+1}+t_n),\quad t_{n-2}+t_{n-1}+t_n] \\ \mathsf{P}_3^b\left(A_{j,k}^{(3)}, \boldsymbol{t}\right) & = & [t_1+t_2+t_3,\quad \max(t_1+t_{j-1}+t_j,\ t_{k-1}+t_k+t_n)] \end{array}$$

For $\boldsymbol{t} \in \mathsf{O}_n^\circ$, a 3-arborescence A with $A = A_k^{(3)}$ (for some $k \in [n-1]$) or $A = A_{j,k}^{(3)}$ (for some $1 < k \leq j-1 \leq n-1$), A corresponds to a vertex of $\Pi(\mathsf{Cyc}_3(\boldsymbol{t}), \boldsymbol{e}_1)$ if and only if $\mathsf{P}_d^f(A, \boldsymbol{t}) \cap \mathsf{P}_d^b(A, \boldsymbol{t}) = \varnothing$.

Proof. This proof is slightly different from the one of Theorem 3.16 because we can not benefit from Lemma 3.15, as $\Pi(\mathsf{Cyc}_3(\boldsymbol{t}), \boldsymbol{e}_1)$ is not the projection of an associahedron. Nevertheless, the same proof than for Theorem 3.16, applying Gordan's lemma to the inequalities of Proposition 3.43, gives that A can be captured on $\boldsymbol{t}$ if and only if $\mathsf{P}_3^f(A, \boldsymbol{t}) \cap \mathsf{P}_3^b(A, \boldsymbol{t}) = \varnothing$ where:

$$\begin{array}{rcl} \mathsf{P}_3^f(A, \boldsymbol{t}) & = & \operatorname{conv}\{t_x + t_y + t_z \ :\ x < y < z \text{ all triples such that } A \text{ imposes } \tau(x,y) > \tau(x,z)\} \\ \mathsf{P}_3^b(A, \boldsymbol{t}) & = & \operatorname{conv}\{t_x + t_y + t_z \ :\ x < y < z \text{ all triples such that } A \text{ imposes } \tau(x,y) < \tau(x,z)\} \end{array}$$

On the one hand, $A_k^{(3)}$ imposes $\tau(x,y) > \tau(x,z)$ for $(x,y,z) \in \{(1,2,i)\}_{i \geq 3} \cup \{(i,i+1,n)\}_{i \leq k-1}$; and $\tau(x,y) < \tau(x,z)$ for $(x,y,z) \in \{(a,a+1,n)\}_{a \geq k}$. Analyzing the minimum and maximum possible sums of triplets gives the desired endpoints of both segments.

On the other hand, $A_{j,k}^{(3)}$ imposes $\tau(x,y) > \tau(x,z)$ for $(x,y,z) \in \{(1,j,i)\}_{i>j} \cup \{(i,i+1,n)\}_{i \geq k}$; and $\tau(x,y) < \tau(x,z)$ for $(x,y,z) \in \{(1,a,j)\}_{a<j} \cup \{(a,a+1,n)\}_{1<a<k}$. Analyzing the minimum and maximum possible sums of triplets give the desired endpoints of both segments. □

This result allows us to determine which 3-arborescences are *universal* in the sense that they correspond to a vertex of $\Pi(\mathsf{Cyc}_3(\boldsymbol{t}), \boldsymbol{e}_1)$ for all $\boldsymbol{t} \in \mathsf{O}_n^\circ$, and to give an inequality description of their realization set otherwise.

Corollary 3.46. *For all $k \in [n-1]$, the 3-arborescence $A_k^{(3)}$ is universal. For $(j,k) \in \{(3,2),(4,2),(n,n-2)\}$, the 3-arborescence $A_{j,k}^{(3)}$ is universal.*

For $1 < k \leq j-1 \leq n-1$ with $(j,k) \notin \{(3,2),(4,2),(n,n-2),(n,n-1)\}$, the 3-arborescence $A_{j,k}^{(3)}$ is not universal, and corresponds to a vertex of $\Pi(\mathsf{Cyc}_3(\boldsymbol{t}), \boldsymbol{e}_1)$ if and only if

$$\boldsymbol{t} \in \mathsf{O}_n^\circ \ \cap\ \left\{ \boldsymbol{t} \in \mathbb{R}^n \ ;\ \begin{array}{rcll} t_{k-1}+t_k+t_n & < & t_1+t_j+t_{j+1} & \text{when } k \neq 2 \text{ and } j \neq n \\ t_1+t_{j-1}+t_j & < & t_k+t_{k+1}+t_n & \end{array} \right\} \subsetneq \mathsf{O}_n^\circ$$

Proof. For all $\boldsymbol{t} \in \mathsf{O}_n^\circ$, and $k \in [n-1]$, it is easily seen that $\mathsf{P}_3^f\left(A_k^{(3)}, \boldsymbol{t}\right)$ and $\mathsf{P}_3^b\left(A_k^{(3)}, \boldsymbol{t}\right)$ do not intersect.

For $\boldsymbol{t} \in \mathsf{O}_n^\circ$ and $1 < k \leq j-1 \leq n-1$, $\mathsf{P}_3^f\left(A_{j,k}^{(3)}, \boldsymbol{t}\right)$ and $\mathsf{P}_3^b\left(A_{j,k}^{(3)}, \boldsymbol{t}\right)$ do not intersect if and only if $t_{k-1}+t_k+t_n < t_1+t_j+t_{j+1}$ and $t_1+t_{j-1}+t_j < t_k+t_{k+1}+t_n$. The first inequality is defined only when $k \neq 2$ and $j \neq n$. This gives the last part of the above corollary.

Furthermore, the above inequalities are redundant with respect to the ones of O_n° if and only if $(j,k) \in \{(3,2),(4,2),(n,n-2)\}$. □

Definition 3.47. For n, the *3-switching arrangement* $\mathcal{H}_n^{(3)}$ is the collection of hyperplanes defined for $1 < k \leq j-1 \leq n-1$ by:

$$H_{j,k} = \{\boldsymbol{t} \in \mathbb{R}^n \ ;\ t_k + t_{k+1} + t_n = t_1 + t_j + t_{j+1}\}$$

Remark that the two inequalities of the above corollary correspond to the hyperplanes $H_{j,k-1}$ and $H_{j-1,k}$. Consequently, the same ideas as for Corollary 3.37 allows us to prove the following main results:

Theorem 3.48. *The number of vertices of $\Pi(\mathsf{Cyc}_3(\boldsymbol{t}), \boldsymbol{e}_1)$ is the same for all $\boldsymbol{t} \in \mathsf{O}_n^\circ \setminus \bigcup_{H \in \mathcal{H}_n^{(3)}} H$.*

Proof. By Corollary 3.46, if $\boldsymbol{t}$ and $\boldsymbol{t}'$ belong to the same maximal cone of $\mathsf{O}_n^\circ \setminus \bigcup_{H\in\mathcal{H}_n^{(3)}} H$, then the 3-arborescences captured on $\boldsymbol{t}$ and $\boldsymbol{t}'$ are the same. Thus the number of vertices of $\Pi(\mathsf{Cyc}_3(\boldsymbol{t}), \boldsymbol{e}_1)$ and $\Pi(\mathsf{Cyc}_3(\boldsymbol{t}'), \boldsymbol{e}_1)$ are the same.

For a maximal cone C of the arrangement $\mathcal{H}_n^{(3)}$, we denote by $\mathcal{A}^{(3)}(\mathsf{C})$ the set of 3-arborescences captured on (any) $\boldsymbol{t} \in \mathsf{C}$. Take two adjacent maximal cones C and C'. Suppose that, for some $1 < k \leq j-1 \leq n-1$ with $(j,k) \notin \{(3,2),(4,2),(n,n-2),(n,n-1)\}$, $A^{(3)}_{j,k} \in \mathcal{A}^{(3)}(\mathsf{C})$ but $A^{(3)}_{j,k} \notin \mathcal{A}^{(3)}(\mathsf{C}')$. Then the hyperplane separating C and C' is either $H_{j-1,k}$ or $H_{j,k-1}$. Suppose it is $H_{j-1,k}$, then $A^{(3)}_{j+1,k-1} \notin \mathcal{A}^{(3)}(\mathsf{C})$ (as C is not on the side of $H_{j-1,k}$ where $A^{(3)}_{j+1,k-1}$ can be captured) but $A^{(3)}_{j+1,k-1} \in \mathcal{A}^{(3)}(\mathsf{C}')$ because C' is on the side of $H_{j-1,k}$ where $A^{(3)}_{j+1,k-1}$ can be captured, and on the same side of $H_{j+1,k-2}$ as C, where $A^{(3)}_{j+1,k-1}$ can be captured. If it were $H_{j,k-1}$, then $A^{(3)}_{j-1,k+1} \in \mathcal{A}^{(3)}(\mathsf{C}) \setminus \mathcal{A}^{(3)}(\mathsf{C}')$ for the same reasons.

As all other 3-arborescences can be captured both in C and C', we deduce that $|\mathcal{A}^{(3)}(\mathsf{C}')| \geq |\mathcal{A}^{(3)}(\mathsf{C})|$. This proves that the cardinal $|\mathcal{A}^{(3)}(\mathsf{C})|$ is the same for all maximal cone C of the hyperplane arrangement $\mathcal{H}_n^{(3)}$ (as the graph of adjacency of its maximal cones is connected). □

Corollary 3.49. *For all $\boldsymbol{t} \in \mathsf{O}_n^\circ \setminus \bigcup_{H\in\mathcal{H}_n^{(3)}} H$, the number of vertices of $\Pi(\mathsf{Cyc}_3(\boldsymbol{t}), \boldsymbol{e}_1)$ is $3n-7$.*

Proof. By Theorem 3.48, it is enough to compute the number of vertices of $\Pi(\mathsf{Cyc}_3(\boldsymbol{t}), \boldsymbol{e}_1)$ for some $\boldsymbol{t} \in \mathsf{O}_n^\circ \setminus \bigcup_{H\in\mathcal{H}_n^{(3)}} H$. Take $\boldsymbol{t}_{lex} = (1, 2, ..., 2^{n-1}) \in \mathsf{O}_n^\circ$, then deciding if $t_a + t_b + t_c < t_x + t_y + t_z$ amount to knowing which triple of indices is lexicographically the greatest between (a,b,c) and (x,y,z). Thus, $\boldsymbol{t}_{lex} \notin \bigcup_{H\in\mathcal{H}_n^{(3)}} H$.

By the inequalities of Corollary 3.46, $A^{(3)}_{j,k}$ is captured on $\boldsymbol{t}_{lex}$ if and only if it falls into one of the following (mutually exclusive) cases:

- $k = 2$ and $j \in [3, n-1]$, accounting for $n-3$ possibilities
- $j = n-1$ and $k \in [3, n-2]$, accounting for $n-4$ possibilities
- $j = n$ and $k = n-2$, accounting for 1 possibility

These, plus the $n-1$ universal arborescences $A^{(3)}_k$ sum up to $3n-7$. □

Example 3.50. For $n = 5$, $\Pi(\mathsf{Cyc}_3(\boldsymbol{t}), \boldsymbol{e}_1)$ are octagons, all but 1 vertex of which correspond to universal 3-arborescences. There are 2 possible such octagons, depending on whether $t_2+t_3+t_5 < t_1+t_4+t_5$ or the converse, see Figure 47.

For $n = 6$, $\Pi(\mathsf{Cyc}_3(\boldsymbol{t}), \boldsymbol{e}_1)$ are 11-gons, all but 3 vertices of which correspond to universal 3-arborescences. There are 5 possible such 11-gons, depending on the position of $\boldsymbol{t}$ with respect to the 3 hyperplanes $\{\boldsymbol{t} \in \mathbb{R}^n \ ; \ t_2+t_3+t_6 = t_1+t_4+t_6\}$, $\{\boldsymbol{t} \in \mathbb{R}^n \ ; \ t_2+t_3+t_6 = t_1+t_5+t_6\}$ and $\{\boldsymbol{t} \in \mathbb{R}^n \ ; \ t_3+t_4+t_6 = t_1+t_5+t_6\}$, see Figure 48.

For $n = 7$, $\Pi(\mathsf{Cyc}_3(\boldsymbol{t}), \boldsymbol{e}_1)$ are 14-gons, all but 5 vertices of which correspond to universal 3-arborescences. There are 12 possible such 14-gons, depending on the position of $\boldsymbol{t}$ with respect to the 6 hyperplanes of $\mathcal{H}_6^{(3)}$.

In general, one can draw the graph whose vertices are all 3-arborescences on n nodes, and where A and A' are linked by an edge when there exists $\boldsymbol{t} \in \mathsf{O}_n^\circ$ such that the vertices of $\Pi(\mathsf{Cyc}_3(\boldsymbol{t}), \boldsymbol{e}_1)$ corresponding to A and A' appear and are linked by an edge. This amounts to consider the graph of "flips" of 3-arborescences: flipping a 3-arborescence $A^{(3)}_k$ gives $A^{(3)}_{k+1}$ for $k \in [n-2]$, flipping $A^{(3)}_{j,k}$ gives either $A^{(3)}_{j+1,k}$ or $A^{(3)}_{j,k+1}$, and flipping $A^{(3)}_{n-1}$ gives either $A^{(3)}_{3,2}$ or $A^{(3)}_{n-2}$. Though tedious, this definition of flips is made clear in the graph depicted in Figure 49 for $n = 7$. All max-slope pivot polytope $\Pi(\mathsf{Cyc}_3(\boldsymbol{t}), \boldsymbol{e}_1)$ correspond to a *great cycle* in this graph. To count these great cycles, we look at the paths from $A^{(3)}_1$ to $A^{(3)}_{n-1}$ that only uses 3-arborescences of the form $A^{(3)}_{j,k}$. These paths are in bijection with Dick paths of length $2(n-3)$, thus they are $\frac{1}{n-2}\binom{2(n-3)}{n-3}$ many (Catalan number). Note that for $n = 5$ and $n = 6$, all such paths do correspond to max-slope

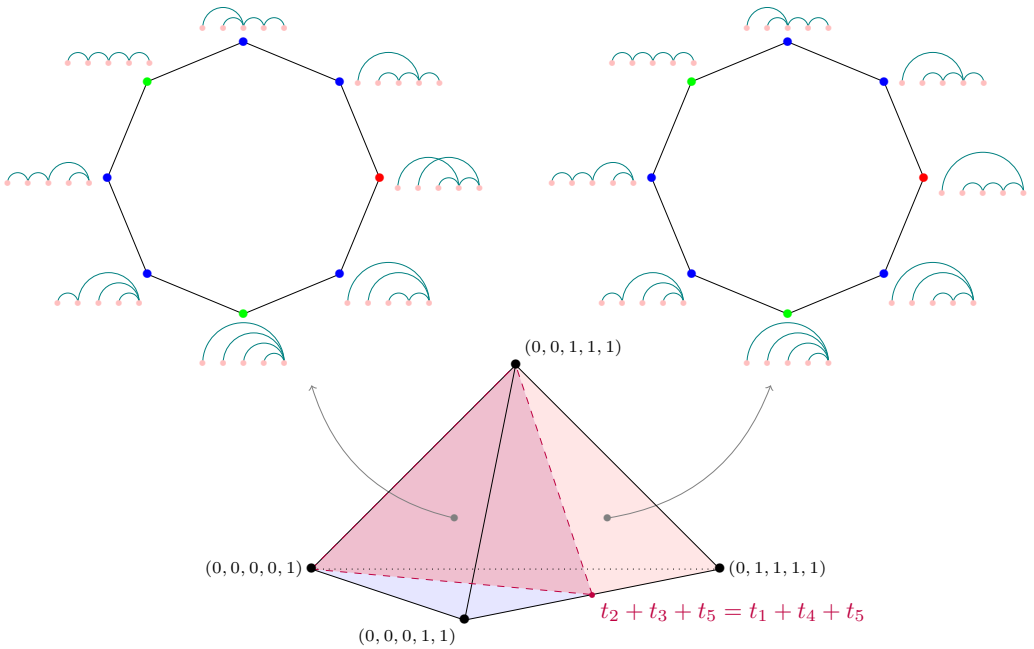

Figure 47: For $n = 5$, $\Pi(\mathsf{Cyc}_3(\boldsymbol{t}), \boldsymbol{e}_1)$ are octagons. Green and blue vertices represent universal 3-arborescences (green are captured by degree 2 polynomials), the red vertex is non-universal. For $\boldsymbol{t} \in \mathsf{O}_5^\circ$ with $t_2 + t_3 + t_5 < t_1 + t_4 + t_5$, the 3-arborescence $A^{(3)}_{4,3}$ can be captured, while $A^{(3)}_{5,2}$ can not (and conversely).

pivot polytopes (in the sense that there exists a $\boldsymbol{t} \in \mathsf{O}_n^\circ$ such that the vertices of $\Pi(\mathsf{Cyc}_3(\boldsymbol{t}), \boldsymbol{e}_1)$ correspond to the 3-arborescences appearing in this path). But for $n = 7$, there are only 12 possible max-slope pivot polytopes: not all 14 paths correspond to a max-slope pivot polytope, only 12 of them do. Again, one can wonder how many combinatorially different $\Pi(\mathsf{Cyc}_3(\boldsymbol{t}), \boldsymbol{e}_1)$ there are for all n.

This concludes this complementary section on 2- and 3-dimensional problems, and closes (almost completely) the case. As per usual, we devote the last sub-section to some perspectives and open questions. This sub-section will concern the general problem for $d \geq 4$, so the readers can forget what they just read and have a look again at Figures 38 to 40 and 43.

3.2.4 Perspectives and open questions

Computational remarks All the objects mentioned in this section have been implemented with Sage, allowing to compute the above examples. There are two possibilities for computing the maximal cones of the subdivision $\boldsymbol{S}_n$ mentioned in Example 3.38, and especially for counting the number of such cones. We say that two maximal cones correspond to two *combinatorially different* cyclic associahedra.

A straightforward way to do so is to take the hyperplane arrangement $\mathcal{H}_n$ and compute the maximal cones it induces, as topes of the corresponding oriented matroid. It is then easy to list the arborescences captured in each tope (it amounts to checking for each 3-arborescence if it respects the inequalities of its realization set), and to count how many different lists we get. To speed up this process, we use the *forcing poset* $\mathcal{F}_n$ of hyperplanes, that is the poset of inclusion of $H^+ \cap \mathsf{O}_n$ for $H \in \mathcal{H}_n$. Indeed, a tope corresponds to a down set of the forcing poset (but not all down sets correspond to topes).

On Figure 50 are the forcing posets $\mathcal{F}_6$ (Left) and $\mathcal{F}_7$ (Right, only the poset structure, without labeling). Quite remarkably, $\mathcal{F}_6$ has 12 down-sets which correspond to the 12 cyclic associahedra of Example 3.38. This explains the cubical structure of the dual graph of the polyhedral subdivision

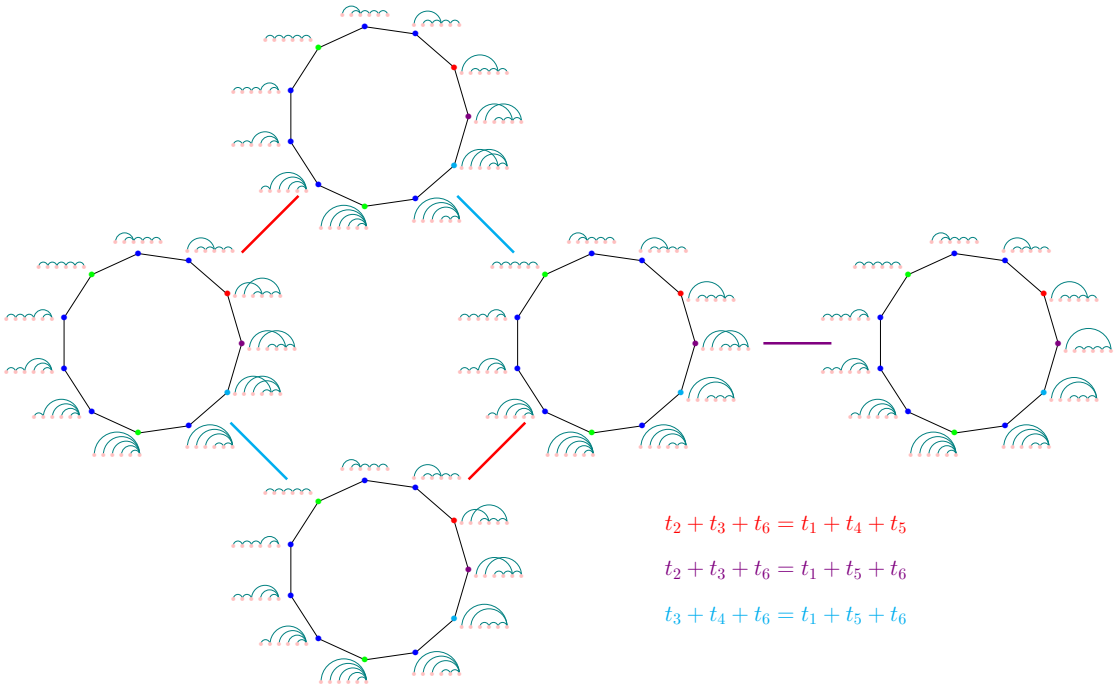

Figure 48: For $n = 6$, $\Pi(\mathsf{Cyc}_3(\boldsymbol{t}), \boldsymbol{e}_1)$ are 11-gons. Each 11-gon correspond to a subcone of O_6° on which its 3-arborescences are precisely the one captured. There are 5 such subcones, and the five colored edges figure the dual graph of this subdivision. For example, two 11-gons are linked by a red thick edge when their 11-gons differ only on the label of the red vertex.

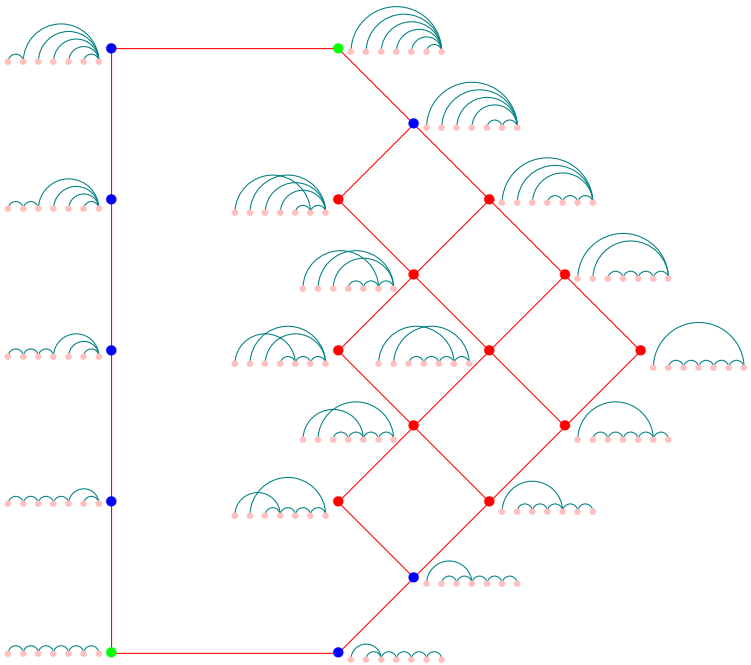

Figure 49: Green and blue dots represent universal arborescences, red dots non-universal ones. Each $\Pi(\mathsf{Cyc}_3(\boldsymbol{t}), \boldsymbol{e}_1)$ for $\boldsymbol{t} \in \mathsf{O}_7^\circ$ correspond to a great circle in this graph. A great circle is composed of the path from the green node to the other one on the left of the picture (using $A_k^{(3)}$s) and a path on the right of the picture (going from top to bottom). Not all great circles correspond to a $\Pi(\mathsf{Cyc}_3(\boldsymbol{t}), \boldsymbol{e}_1)$.

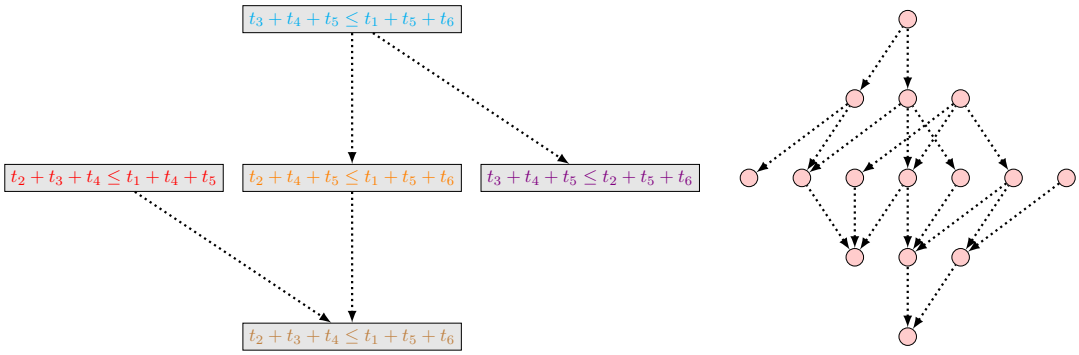

Figure 50: The forcing posets $\mathcal{F}_6$ (Left) and $\mathcal{F}_7$ (Right). Having only 1 element, $\mathcal{F}_5$ is not drawn.

for $n = 6$ in Figure 43: oriented from left to right and top to bottom, it is the graph of a lattice of ideals, which is a distributive lattice, hence cubical.

Unfortunately, not all down-sets of $\mathcal{F}_7$ do correspond to topes of the polyhedral subdivision for $n = 7$: $\mathcal{F}_7$ has 336 down-sets whereas there are only 187 topes in the polyhedral subdivision, each of them corresponding to a combinatorially different cyclic associahedron. This comes from the fact that being in some subsets of half-spaces forces to be in some other subsets, whereas the forcing poset only records if being in one half-space forces to be in another. But trying to construct the forcing relation for subsets of half-spaces would become impracticable, as there are already 15 elements in $\mathcal{F}_7$ (so 2^{15} subsets) and 35 in $\mathcal{F}_8$ (so 2^{35} subsets).

The failure of this first method advocates for a new one. Going back to Example 3.23, Corollary 3.37 implies that all cyclic associahedra come from a great cycle in the sub-graph of the Tamari graph induced by the non-crossing arborescences A with $\mu(A) \le 3$ (*i.e.* the graphs pictured in Figures 38 and 39 and their counterparts for greater n). We can run through all these great cycles, and for each of them compute the intersection of $\mathcal{T}_3(A)$ for the non-crossing arborescences in the great cycle. The family of arborescences forming the great cycle correspond to a cyclic associahedron if and only if this intersection is non-empty. This algorithmic solution gives the number of combinatorially different cyclic associahedra for $n = 8$ by testing "only" 33592 great cycles.

n	5	6	7	8
number of combinatorially different cyclic associahedra $\mathsf{Asso}_2(\boldsymbol{t})$	1	12	187	6179

Assets and limits of the current approach, open questions This computer experiment raises the following natural open question: How many combinatorially different cyclic associahedra $\mathsf{Asso}_2(\boldsymbol{t})$ are there for $n \ge 9$? We have proven that all cyclic associahedra $\mathsf{Asso}_2(\boldsymbol{t})$ have the same number of vertices $\binom{n}{2} - 1$ by Corollary 3.37. We know how to determine if a non-crossing arborescence A satisfies $\mu(A, \boldsymbol{t}) \le 3$ or not (by checking if a set of linear inequality has a solution, *i.e.* by solving a linear problem), but we do not know how to efficiently compute the number of combinatorially different cyclic associahedra.

On the other hand, the works presented so far only deal with the case $d \le 3$. Numerous questions are still open for $d \ge 4$. Indeed, Theorem 3.16 gives a way to check if, for a given $\boldsymbol{t}$, a non-crossing arborescence A satisfies $\mu(A, \boldsymbol{t}) \le \boldsymbol{t}$, but it remains difficult to compute $\mathcal{T}_d(A)$. To do so, one would need to determine for which $\boldsymbol{t}$ do some $(d-2)$-dimensional polytopes intersect, but these polytopes have coordinates of degree $d-2$ in $\boldsymbol{t}$, making the question (at least) as hard as computing a semi-algebraic set of degree $d-2$. With the help of the cylindrical algebraic decomposition, see [BPR06, Chapter 5], one can hope for dealing with the case $d = 4$ and $n = 6$, but going higher would require a better mathematical understanding of our problem.

Nonetheless, computer experiments indicate that the number of vertices of $\mathsf{Asso}_{d-1}(\boldsymbol{t})$ depends on $\boldsymbol{t}$ for $d = 4$. Moreover, given a set $\mathcal{A}$ of non-crossing arborescences, it is unclear whether the common realization set $\bigcap_{A \in \mathcal{A}} \mathcal{T}_d(A)$ is connected or not, and we believe that there exists $\mathcal{A}$ such that it is not connected, even for $d = 4$ (but have not found an example yet).

3.3 Max-slope pivot polytopes of products of polytopes

This section is an ongoing work on a conjecture of Vincent Pilaud and Raman Sanyal.

In the previous section, we have computed the max-slope pivot polytopes of cyclic polytopes. Especially, if one reviews the computation, he or she will notice that the key objects are the slopes in the plane $(\boldsymbol{c}, \boldsymbol{\omega})$ between the projection of adjacent vertices $\boldsymbol{u}, \boldsymbol{v} \in V(\mathsf{P})$, namely $\frac{\langle \boldsymbol{\omega}, \boldsymbol{u}-\boldsymbol{v}\rangle}{\langle \boldsymbol{c}, \boldsymbol{u}-\boldsymbol{v}\rangle}$. The comparisons between these slopes determine the arborescence associated to $\boldsymbol{\omega}$, and, for fixed $\boldsymbol{c}$, $\boldsymbol{u}$ and $\boldsymbol{v}$, these slopes are linear with respect to $\boldsymbol{\omega}$. In the present section, we will emphasize this idea by considering the partially ordered set that records only these comparisons and forgets the exact values of the slopes. Not only will this grant us, in Section 3.3.1, a second proof that the max-slope pivot polytope of the standard cube is the permutahedron [BDLLS22], and that the max-slope pivot polytope of a simplex is an associahedron [BDLLSon], but it will also give access, in Section 3.3.2, to the max-slope pivot polytope of a product of simplices (and grasp some hint about products of polytopes in general).

Generalized permutahedra will be at the center of this part, as we unveil the link between the normal fan of the max-slope pivot polytope and the braid fan. Besides Section 3.1 which introduces the preliminary notions concerning max-slope pivot rule polytopes, the useful definitions on pre-orders and braid fans are presented in Sections 1.1 and 1.2.3. We will directly use the notations defined in these preliminaries.

The watchword of this section is that max-slope pivot rule polytopes can be embedded in the braid fan and thought of as akin to generalized permutahedra. As a consequence, we will be able to detail max-slope pivot polytopes of products of simplices and prove that they are linked to the notion of shuffle defined in [CP22] on generalized permutahedra. In particular, this allows us to give new families of realizations of the multiplihedron and the constrainahedron in Example 3.75. These polytopes are generalizations of the permutahedron and the associahedron. Especially, the *constrainahedron* was introduced by Bottman and Poliakova [Bot19, Pol21] in order to study higher version of the A_∞ operad. The vertices of the constrainahedron are associated to bracketing on the 2-dimensional $m \times n$-grid, whereas the vertices of the usual associahedron correspond to usual bracketing (see Section 1.2.4). As to the *multiplihedron*, its vertices are in bijection with m-painted binary n-trees, and its combinatorics arises from the study of maps between A_∞-algebras, see [For08] for an historical presentation of the subject.

In this section, the central tools are only basic linear algebra (namely linear maps and dimensions of vector spaces), and (shuffle of) partially ordered set. Although these notions are well known to the reader, the notions will feel heavy and unwieldy, making the proofs technical. The reader is advised to first read the theorems and examples, and then to keep in mind that the idea is to prove that what the framework suggests is indeed true.

We start by exposing the general theory of how to embed max-slope pivot polytopes into the realm of generalized permutahedra. To this end, we need an elementary lemma:

Lemma 3.51. *The projection $\pi : \mathbb{R}^n \to \mathbb{R}^{n-1}$ that forgets the last coordinate sends the braid fan $\mathcal{B}_n$ onto the braid fan $\mathcal{B}_{n-1}$. For a surjection α of $[n-1]$, the pre-image of the cone C_α is exactly the union of cones: $\pi^{-1}(\mathsf{C}_\alpha) = \bigcup_{\sigma \text{ extends } \alpha} \mathsf{C}_\sigma$.*

Proof. This fact is straightforward from the definition of C_σ:

$$\mathsf{C}_\sigma = \left\{ \boldsymbol{x} \in \mathbb{R}^n \; ; \quad \begin{array}{lll} x_i < x_j & \text{if} & \sigma(i) < \sigma(j) \\ x_i = x_j & \text{if} & \sigma(i) = \sigma(j) \end{array} \right\}$$

□

As we want to discuss max-slope pivot polytopes as a whole and not only their vertices, we first detail the combinatorial interpretation of the faces of the max-slope pivot polytope, see [BDLLS22, Section 5]. For the rest of this discussion, we fix a linear program $(\mathsf{P}, \boldsymbol{c})$, on a polytope P of dimension d, n its number of vertices, and m its number of edges. As before, the set of vertices of P is $V(\mathsf{P})$, and $\boldsymbol{v}_{\text{opt}}$ is the vertex maximizing $\langle \boldsymbol{v}, \boldsymbol{c}\rangle$. Besides, $E_{\boldsymbol{c}}(\mathsf{P})$ will be the set of $\boldsymbol{c}$-improving edges of P, that is edges $\boldsymbol{uv}$ of P with $\langle \boldsymbol{u}, \boldsymbol{c}\rangle < \langle \boldsymbol{v}, \boldsymbol{c}\rangle$. As always: $\tau_{\boldsymbol{\omega}}(\boldsymbol{u}, \boldsymbol{v}) = \frac{\langle \boldsymbol{\omega}, \boldsymbol{u}-\boldsymbol{v}\rangle}{\langle \boldsymbol{c}, \boldsymbol{u}-\boldsymbol{v}\rangle}$

Definition 3.52. A *multi-arborescence* $\mathcal{A}$ is a function $\mathcal{A} : V(\mathsf{P}) \smallsetminus \{\boldsymbol{v}_{\mathrm{opt}}\} \to 2^{V(\mathsf{P})}$ such that $\mathcal{A}(\boldsymbol{v})$ is a non-empty subset of $\boldsymbol{c}$-improving neighbors of $\boldsymbol{v}$. By convention $\mathcal{A}(\boldsymbol{v}_{\mathrm{opt}}) = \{\boldsymbol{v}_{\mathrm{opt}}\}$ when needed.

A secondary direction $\boldsymbol{\omega}$ *captures* the following multi-arborescence (where "Argmax" designates the set of maximizers of the studied quantity) :

$$\mathcal{A}^{\boldsymbol{\omega}}(\boldsymbol{v}) = \mathrm{Argmax}\left\{ \frac{\langle \boldsymbol{\omega}, \boldsymbol{u} - \boldsymbol{v} \rangle}{\langle \boldsymbol{c}, \boldsymbol{u} - \boldsymbol{v} \rangle} \ ; \ \boldsymbol{uv} \in E_{\boldsymbol{c}}(\mathsf{P}) \right\}$$

A multi-arborescence $\mathcal{A}$ is *coherent* when there exists $\boldsymbol{\omega}$ such that $\mathcal{A} = \mathcal{A}^{\boldsymbol{\omega}}$, and we denote $\tau_{\boldsymbol{\omega}}(\mathcal{A}(\boldsymbol{u})) = \tau_{\boldsymbol{\omega}}(\boldsymbol{u}, \boldsymbol{v})$ for any[9] $\boldsymbol{v} \in \mathcal{A}(\boldsymbol{u})$.

We say that a multi-arborescence $\mathcal{A}$ *refines* a multi-arborescence $\mathcal{A}'$ when $\mathcal{A}(\boldsymbol{v}) \subseteq \mathcal{A}'(\boldsymbol{v})$ for all $\boldsymbol{v} \in V(\mathsf{P})$. In this case, we denote by $\mathcal{A} \subseteq \mathcal{A}'$ this relation, and by $\mathfrak{A}$ the corresponding partially ordered set completed by an arbitrary minimal element $\varnothing$. The following theorem gives access to the face lattice of the max-slope pivot polytope.

Theorem 3.53. ([BDLLS22, Theorem 5.4]) *For a linear program $(\mathsf{P}, \boldsymbol{c})$, the lattice of coherent multi-arborescences $\mathfrak{A}$ is isomorphic to the face lattice of the max-slope pivot polytope $\Pi(\mathsf{P}, \boldsymbol{c})$.*

Fix a linear program $(\mathsf{P}, \boldsymbol{c})$ and a coherent multi-arborescence $\mathcal{A}$ on it, we denote $\mathsf{F}_{\mathcal{A}}$ the corresponding face in the max-slope pivot polytope $\Pi(\mathsf{P}, \boldsymbol{c})$. By (a refined version of) Theorem 3.1, we know that the normal cone at $\mathsf{F}_{\mathcal{A}}$ is precisely the cone of $\boldsymbol{\omega}$ that captures $\mathcal{A}$. We call $\mathcal{N}(\mathcal{A})$ this cone, and set $\mathcal{N}(\mathcal{A}) = \varnothing$ when $\mathcal{A}$ is not coherent.

In order to know what multi-arborescence a given $\boldsymbol{\omega}$ captures, one does not need the exact value of $\boldsymbol{\omega}$, but only the comparisons between the slopes $\boldsymbol{\omega}$ gives to each improving edge $\boldsymbol{uv}$ of P (when projecting this edge into the plane $(\boldsymbol{c}, \boldsymbol{\omega})$). This invites us to define the two following pre-orders.

Definition 3.54. For a given $\boldsymbol{\omega} \in \mathbb{R}^d$, its *slope vector* is $\theta(\boldsymbol{\omega}) := \big(\tau_{\boldsymbol{\omega}}(\boldsymbol{u}, \boldsymbol{v}) \ ; \ \boldsymbol{uv} \in E_{\boldsymbol{c}}(\mathsf{P})\big) \in \mathbb{R}^{E_{\boldsymbol{c}}(\mathsf{P})}$.

Moreover, a given $\boldsymbol{\omega}$ induces a pre-order on $E_{\boldsymbol{c}}(\mathsf{P})$, called its *slope pre-order*, by considering $\boldsymbol{uv} \preccurlyeq_{\boldsymbol{\omega}} \boldsymbol{u'v'}$ when $\tau_{\boldsymbol{\omega}}(\boldsymbol{u}, \boldsymbol{v}) \leq \tau_{\boldsymbol{\omega}}(\boldsymbol{u'}, \boldsymbol{v'})$, or equivalently $\theta(\boldsymbol{\omega})_{\boldsymbol{uv}} \leq \theta(\boldsymbol{\omega})_{\boldsymbol{u'v'}}$.

The knowledge of the slope pre-order of $\boldsymbol{\omega}$ fully determines which multi-arborescence it captures, and this pre-order can be retrieved from comparison between coordinates of its slope vector. Note that the map $\boldsymbol{\omega} \mapsto \theta(\boldsymbol{\omega})$ is a linear map.

Furthermore, if $\boldsymbol{\omega} \in \mathbb{R}^d$ captures a multi-arborescence $\mathcal{A}$, it necessarily satisfies some slope inequalities, *i.e.* certain relations of its slope pre-order can be deduced from the capture of $\mathcal{A}$. For instance, if $\boldsymbol{\omega}$ captures $\mathcal{A}$, then the improving edges $\boldsymbol{uv}$ with $\boldsymbol{v} \in \mathcal{A}(\boldsymbol{u})$ are greater (for the slope pre-order of $\boldsymbol{\omega}$) than any improving edge $\boldsymbol{uv'}$. And we have seen in the previous Section 3.2 that Lemma 3.5 allows us to compare other slopes between them thanks to the triangles in the graph G_{P}.

We thus endow $\mathcal{A}$ with a pre-order of its own:

Definition 3.55. A multi-arborescence $\mathcal{A}$ induces an *utter slope pre-order* on the set $E_{\boldsymbol{c}}(\mathsf{P})$ by $\boldsymbol{uv} \preccurlyeq_{\mathcal{A}} \boldsymbol{u'v'}$ when $\tau_{\boldsymbol{\omega}}(\boldsymbol{u}, \boldsymbol{v}) \leq \tau_{\boldsymbol{\omega}}(\boldsymbol{u'}, \boldsymbol{v'})$ for all $\boldsymbol{\omega} \in \mathbb{R}^d$ capturing $\mathcal{A}$. Said equivalently:

$$\boldsymbol{uv} \preccurlyeq_{\mathcal{A}} \boldsymbol{u'v'} \iff \forall \boldsymbol{\omega} \in \mathcal{N}(\mathcal{A}),\ \boldsymbol{uv} \preccurlyeq_{\boldsymbol{\omega}} \boldsymbol{u'v'}$$

It is then immediate to see that:

Proposition 3.56. *A given $\boldsymbol{\omega} \in \mathbb{R}^d$ captures a multi-arborescence $\mathcal{A}$ if and only if $\preccurlyeq_{\boldsymbol{\omega}}$ extends $\preccurlyeq_{\mathcal{A}}$.*

The drawback of the utter slope pre-order of $\mathcal{A}$ is that it might encapsulate geometric constraints, while we would like to only care about the combinatorial constraints. Indeed, one could think that the utter slope pre-order is obtained by first enforcing, for all $\boldsymbol{u}$, that $\boldsymbol{uv'} \preccurlyeq_{\mathcal{A}} \boldsymbol{uv}$ when $\boldsymbol{v} \in \mathcal{A}(\boldsymbol{u})$, and then repeatedly applying Lemma 3.5 to deduce all possible slope inequalities.

[9] Note that the slope does not depend on $\boldsymbol{v} \in \mathcal{A}(\boldsymbol{u})$ by definition of the multi-arborescence.

Nevertheless, this is false: it can happen that all $\boldsymbol{\omega}$ capturing $\mathcal{A}$ respect a slope inequality that cannot be deduced by Lemma 3.5, see Example 3.76 and Figure 54(Bottom Right).

The other inconvenient of the slope vector is that it compares all the edges: not only have we seen that it implies comparisons that cannot be read from the multi-arborescence, but it also involves the slope vector which live in $\mathbb{R}^{E_{\boldsymbol{c}}(\mathsf{P})}$. We would like to keep less information and consequently embed our problem in a smaller dimension. To this end, we restrict the utter slope pre-order to the edges that are used by the multi-arborescence (and forget the other ones), this is easier done by considering the vertices of P instead of its edges:

Definition 3.57. For a multi-arborescence $\mathcal{A}$ and a given $\boldsymbol{\omega} \in \mathbb{R}^d$, the associated *restricted slope vector* is $\vartheta_{\mathcal{A}}(\boldsymbol{\omega}) := \big(\tau_{\boldsymbol{\omega}}(\mathcal{A}(\boldsymbol{v})) \ ; \ \boldsymbol{v} \in V(\mathsf{P}) \smallsetminus \{\boldsymbol{v}_{\text{opt}}\}\big) \in \mathbb{R}^{V(\mathsf{P})\smallsetminus\{\boldsymbol{v}_{\text{opt}}\}}$. A multi-arborescence $\mathcal{A}$ induces an *adapted slope pre-order* on the set $V(\mathsf{P})\smallsetminus\{\boldsymbol{v}_{\text{opt}}\}$ by $\boldsymbol{u} \trianglelefteq_{\mathcal{A}} \boldsymbol{v}$ when $\tau_{\boldsymbol{\omega}}(\mathcal{A}(\boldsymbol{u})) \leq \tau_{\boldsymbol{\omega}}(\mathcal{A}(\boldsymbol{v}))$ for all $\boldsymbol{\omega} \in \mathbb{R}^d$ capturing $\mathcal{A}$, or equivalently $\vartheta_{\mathcal{A}}(\boldsymbol{\omega})_{\boldsymbol{uv}} \leq \vartheta_{\mathcal{A}}(\boldsymbol{\omega})_{\boldsymbol{u'v'}}$ for all $\boldsymbol{\omega} \in \mathcal{N}(\mathcal{A})$.

Finally, we define a map to encompasses all the restricted slope vectors. All these maps are illustrated in Figure 51.

Definition 3.58. The *adapted slope vector* associated to $\boldsymbol{\omega} \in \mathbb{R}^d$ is defined by $\vartheta(\boldsymbol{\omega}) = \vartheta_{\mathcal{A}^{\boldsymbol{\omega}}}(\boldsymbol{\omega})$.

In the utter slope pre-order, the improving edges $\boldsymbol{uv}$ with $\boldsymbol{v} \in \mathcal{A}(\boldsymbol{u})$ are greater than any improving edge $\boldsymbol{uv'}$. Conversely, given a pre-order on $E_{\boldsymbol{c}}(\mathsf{P})$, such that for all $\boldsymbol{u} \in V(\mathsf{P})$ the maxima of $\big(\boldsymbol{uv}\big)_{\boldsymbol{v}\ ;\ \boldsymbol{uv}\in E_{\boldsymbol{c}}(\mathsf{P})}$ are equivalent, then this pre-order determines a unique multi-arborescence. Nevertheless, this is no longer true for the adapted slope pre-order: we will see that several coherent multi-arborescences share the same adapted slope pre-order.

Still, the adapted slope pre-order is a restriction of the utter one:

Lemma 3.59. *For a multi-arborescence $\mathcal{A}$ and a vertex $\boldsymbol{u} \in V(\mathsf{P}) \smallsetminus \{\boldsymbol{v}_{opt}\}$, fix arbitrarily a representative $\boldsymbol{v_u} \in \mathcal{A}(\boldsymbol{u})$. The map $\boldsymbol{u} \mapsto \boldsymbol{uv_u}$ is an injective (pre)order preserving map from the adapted pre-order to the utter pre-order.*

Proof. The map $\boldsymbol{u} \mapsto \boldsymbol{uv_u}$ is clearly injective. As $\tau_{\boldsymbol{\omega}}(\mathcal{A}(\boldsymbol{u})) = \tau_{\boldsymbol{\omega}}(\boldsymbol{u}, \boldsymbol{v_u})$ by definition, this map is (pre)order preserving. □

The utter and the adapted slope pre-orders are linked to the braid fan. Indeed, for each of them, we directly compare the slopes. The maps $\theta : \mathbb{R}^d \to \mathbb{R}^m$, $\vartheta_{\mathcal{A}} : \mathbb{R}^d \to \mathbb{R}^{n-1}$, and $\vartheta : \mathbb{R}^d \to \mathbb{R}^{n-1}$ will play a crucial role in what follows. The next theorem will show that the two first maps embed the pivot polytope into the realm of generalized permutahedra and braid fans, even though they have the undeniable handicap of raising the dimension. The last map ϑ is not, in general, well-behaved, but it will reveal powerful once the aforementioned handicap dealt with.

Definition 3.60. In a fan $\mathcal{F}$, a *great cone* is a cone that can be written as the union of cones of $\mathcal{F}$.

A fan $\mathcal{G}$ is *embedded into* a fan $\mathcal{F}$ when the cones of $\mathcal{G}$ are great cones of $\mathcal{F}$.

In the braid fan $\mathcal{B}_n$, a *pre-order cone* is a great cone associated to a pre-order $\leq$ and defined as $\mathsf{C}_{\leq} = \bigcup_{\sigma \text{ extends } \leq} \mathsf{C}_{\sigma}$ for σ surjection.

Theorem 3.61. *Fix a linear program $(\mathsf{P}, \boldsymbol{c})$, with $n = |V(\mathsf{P})|$ and $m = |E_{\boldsymbol{c}}(\mathsf{P})|$.*

(a) The map $\theta : \mathbb{R}^d \to \mathbb{R}^m$ is an injective linear map that sends the normal fan $\mathcal{N}_{\Pi(\mathsf{P},\boldsymbol{c})}$ of $\Pi(\mathsf{P}, \boldsymbol{c})$ onto a (complete) fan $\theta\big(\mathcal{N}_{\Pi(\mathsf{P},\boldsymbol{c})}\big)$ embedded into the sub-braid fan $\mathcal{B}_m \cap Im(\theta)$, inside $\mathbb{R}^m$. Moreover, a cone $\theta(\mathcal{N}(\mathcal{A}))$ is the intersection of $Im(\theta)$ with the pre-order cone $\mathsf{C}_{\preccurlyeq_{\mathcal{A}}}$.

(b) For a given multi-arborescence $\mathcal{A}$, the map $\vartheta_{\mathcal{A}} : \mathbb{R}^d \to \mathbb{R}^{n-1}$ is a linear map that sends the cone $\mathcal{N}(\mathcal{A})$ onto a great cone of the sub-braid fan $\mathcal{B}_{n-1} \cap Im(\vartheta_{\mathcal{A}})$ inside $\mathbb{R}^{n-1}$. Moreover, the cone $\vartheta_{\mathcal{A}}(\mathcal{N}(\mathcal{A}))$ is the intersection of $Im(\vartheta_{\mathcal{A}})$ with the pre-order cone $\mathsf{C}_{\trianglelefteq_{\mathcal{A}}}$.

Remark 3.62. A sub-braid fan is not necessary a braid fan: it is only a sub-fan of a braid fan, that is the intersection of a braid fan with a linear space (usually of lower dimension).

Proof of Theorem 3.61. (a) As the coordinate of $\theta(\boldsymbol{\omega})$ on $\boldsymbol{uv}$ is $\frac{\langle \boldsymbol{\omega}, \boldsymbol{v}-\boldsymbol{u}\rangle}{\langle \boldsymbol{c}, \boldsymbol{v}-\boldsymbol{u}\rangle}$, it is linear in $\boldsymbol{\omega}$. Furthermore, if $\theta(\boldsymbol{\omega}) = \mathbf{0}$, then $\boldsymbol{\omega}$ is orthogonal to all edges of P, so $\boldsymbol{\omega} = \mathbf{0}$ as P has dimension d. Consequently, θ is an injective linear map.

Fix a cone C in $\theta\big(\mathcal{N}_{\Pi(\mathsf{P},\boldsymbol{c})}\big)$ and consider its pre-image: by injectivity, it is a cone $\mathcal{N}(\mathcal{A})$ for some multi-arborescence $\mathcal{A}$. By Proposition 3.56, a vector $\boldsymbol{\omega} \in \mathbb{R}^d$ belongs to $\mathcal{N}(\mathcal{A})$ if and only if the slope pre-order of $\boldsymbol{\omega}$ is an extension of the utter slope pre-order of $\mathcal{A}$. This is equivalent to requiring that the entries of the slope vector $\theta(\boldsymbol{\omega})$ respect coordinate-wise equalities and inequalities. Consequently, $\boldsymbol{\omega} \in \mathcal{N}(\mathcal{A})$ if and only if $\theta(\boldsymbol{\omega})$ belongs to one of the cones C_σ for σ an extension of the utter slope pre-order, *i.e.* $\mathsf{C} = \mathrm{Im}(\theta) \cap \bigcup_{\sigma \text{ extends } \preccurlyeq_{\mathcal{A}}} \mathsf{C}_\sigma$. As each cone of $\theta\big(\mathcal{N}_{\Pi(\mathsf{P},\boldsymbol{c})}\big)$ is a union of cones of $\mathcal{B}_m$ intersected with $\mathrm{Im}(\theta)$, the embedding is proven.

(b) For a multi-arborescence $\mathcal{A}$ and a vertex $\boldsymbol{u} \in V(\mathsf{P}) \smallsetminus \{\boldsymbol{v}_{\mathrm{opt}}\}$, fix arbitrarily a representative $\boldsymbol{v_u} \in \mathcal{A}(\boldsymbol{u})$, then $\tau_{\boldsymbol{\omega}}(\mathcal{A}(\boldsymbol{u})) = \tau_{\boldsymbol{\omega}}(\boldsymbol{u}, \boldsymbol{v_u})$. Consider the projection $\pi_{\mathcal{A}} : \mathbb{R}^{E_{\boldsymbol{c}}(\mathsf{P})} \to \mathbb{R}^{V(\mathsf{P}) \smallsetminus \{\boldsymbol{v}_{\mathrm{opt}}\}}$ that forgets all coordinates but the ones associated to $(\boldsymbol{u}, \boldsymbol{v_u})$ for $\boldsymbol{u} \in V(\mathsf{P}) \smallsetminus \{\boldsymbol{v}_{\mathrm{opt}}\}$. Then, by definition, $\vartheta_{\mathcal{A}} = \pi_{\mathcal{A}} \circ \theta$, and $\pi_{\mathcal{A}}$ projects the cone $\theta(\mathcal{N}(\mathcal{A}))$ of $\theta\big(\mathcal{N}_{\Pi(\mathsf{P},\boldsymbol{c})}\big)$ onto the cone $\vartheta_{\mathcal{A}}(\mathcal{N}(\mathcal{A}))$. On top of that, by Lemma 3.51, this projection $\pi_{\mathcal{A}}$ projects $\mathcal{B}_m$ onto (a fan linearly isomorphic to) $\mathcal{B}_{n-1}$. Hence, $\vartheta_{\mathcal{A}}(\mathcal{N}(A))$ is a union of cones of $\mathcal{B}_{n-1}$. More precisely, $\vartheta_{\mathcal{A}}(\mathcal{N}(\mathcal{A})) = \mathrm{Im}(\vartheta_{\mathcal{A}}) \cap \bigcup_{\sigma \text{ extends } \preccurlyeq_{\mathcal{A}}} \pi_{\mathcal{A}}\big(\mathsf{C}_\sigma\big)$. As the projection $\pi_{\mathcal{A}}$ forgets all but the coordinates on $\boldsymbol{uv_u}$, Lemma 3.59 ensures that $\pi_{\mathcal{A}}\big(\mathsf{C}_\sigma\big) = \mathsf{C}_\alpha$ for some α that extends $\trianglelefteq_{\mathcal{A}}$, *i.e.* $\vartheta_{\mathcal{A}}(\mathcal{N}(A)) = \mathrm{Im}(\vartheta_{\mathcal{A}}) \cap \bigcup_{\alpha \text{ extends } \trianglelefteq_{\mathcal{A}}} \mathsf{C}_\alpha$. □

Remark 3.63. If P is not full dimensional but embedded into higher dimension, then the kernel of θ is the sub-space orthogonal to the affine hull of P. This does not change the core of the following results, but would overburden the notations.

In general, $\theta\big(\mathcal{N}_{\Pi(\mathsf{P},\boldsymbol{c})}\big)$ is not a complete fan in dimension m. As such, it does not coarsen the braid fan $\mathcal{B}_m$, and $\Pi(\mathsf{P}, \boldsymbol{c})$ is not a deformed permutahedron (in the sense of Section 2). Nonetheless, when Q is a projection of P, then $\mathcal{N}_{\mathsf{Q}}$ is the intersection of $\mathcal{N}_{\mathsf{P}}$ by a sub-space, see [Zie98, Lemma 7.11]. This motivates the following conjecture.

Conjecture 3.64. *For all polytopes $\mathsf{P} \subset \mathbb{R}^d$ with m edges, and objective function $\boldsymbol{c} \in \mathbb{R}^d$, the max-slope pivot polytope $\Pi(\mathsf{P}, \boldsymbol{c})$ is the orthogonal projection of a generalized permutahedron whose normal fan coarsens $\mathcal{B}_m$.*

The projection hinted at in the above conjecture would be the orthogonal projection onto $\mathrm{Im}(\theta)$. If a generalized permutahedron R exists that answers the conjecture, its normal fan $\mathcal{N}_R$ would satisfy $\mathcal{N}_{\mathsf{R}} \cap \mathrm{Im}(\theta) = \theta\big(\mathcal{N}_{\Pi(\mathsf{P},\boldsymbol{c})}\big)$. A natural way to introduce $\mathcal{N}_{\mathsf{R}}$ (as a coarsening of the braid fan $\mathcal{B}_m$) would be to require the maximal cones of $\mathcal{N}_{\mathsf{R}}$ to be exactly $\mathsf{C}_{\preccurlyeq_{\mathcal{A}}} = \bigcup_{\sigma \text{ extends } \preccurlyeq_{\mathcal{A}}} \mathsf{C}_\sigma$ for $\mathcal{A}$ a multi-arborescence on P, but two problems occur. Firstly, it is not mandatory, in general, that all σ extend a $\preccurlyeq_{\mathcal{A}}$ for some multi-arborescence $\mathcal{A}$: in order to properly define the coarsening $\mathcal{N}_{\mathsf{R}}$, one would need to choose what to do with the cones C_σ for σ that does not extend a $\preccurlyeq_{\mathcal{A}}$. On the other hand, it is not clear if there exists a way to choose this coarsening such that $\mathcal{N}_{\mathsf{R}}$ is a fan, and even less clear how to guarantee its polytopality.

Another consequence of the non-completeness of $\theta\big(\mathcal{N}_{\Pi(\mathsf{P},\boldsymbol{c})}\big)$ inside $\mathcal{B}_m$ is that it may happen that $\theta(\mathcal{N}(\mathcal{A}))$ does not intersect a cone C_σ, even though σ extends $\preccurlyeq_{\mathcal{A}}$. This implies that given a multi-arborescence $\mathcal{A}$ and a surjection σ that extends the utter slope pre-order $\preccurlyeq_{\mathcal{A}}$, it can be impossible to find $\boldsymbol{\omega}$ that captures $\mathcal{A}$ with slope pre-order σ.

To confront this non-completeness, one would like to drop dimension, and consider, for instance, the map ϑ, as it goes into $\mathbb{R}^{V(\mathsf{P}) \smallsetminus \{\boldsymbol{v}_{\mathrm{opt}}\}}$ instead of $\mathbb{R}^{E_{\boldsymbol{c}}(\mathsf{P})}$. Although the map θ is linear on the whole normal fan of $\Pi(\mathsf{P}, \boldsymbol{c})$, the map $\vartheta_{\mathcal{A}}$ depends on the chosen multi-arborescence $\mathcal{A}$. Therefore, even though two cones $\vartheta_{\mathcal{A}}(\mathcal{N}(\mathcal{A}))$ and $\vartheta_{\mathcal{A}'}(\mathcal{N}(\mathcal{A}'))$ live in the same braid fan $\mathcal{B}_{n-1}$, they may lie in different sub-spaces $\mathrm{Im}(\vartheta_{\mathcal{A}})$ and $\mathrm{Im}(\vartheta_{\mathcal{A}'})$. Moreover, they may also intersect, and the collection of cones $\big(\vartheta_{\mathcal{A}}(\mathcal{N}(\mathcal{A}))\big)$ for $\mathcal{A}$ a coherent multi-arborescence is not a fan in general. In a word: the map ϑ is not an injective (piece-wise) linear map in general.

Yet, Theorem 3.61 embeds max-slope pivot polytopes into the realm of generalized permutahedra. In particular, this allows us to study the capture of a multi-arborescence as a purely

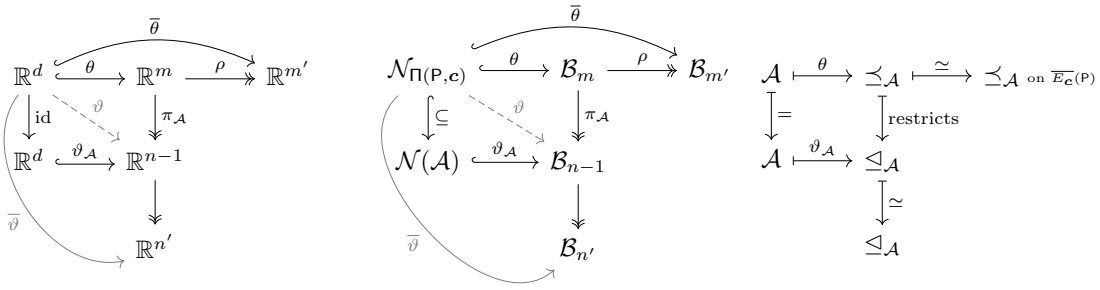

Figure 51: (Middle) The linear maps and projections that embeds the normal fan of $\Pi(\mathsf{P}, \boldsymbol{c})$ into braid fans of different dimensions. (Left) The real vector spaces these maps have for domains. (Right) Utter and adapted pre-orders associated to the multi-arborescence, and their restrictions.

combinatorial phenomenon. Before giving three different applications that benefits from this approach, we deal with parallelisms. As parallel edges always have the same slope when projected onto the plane $(\boldsymbol{c}, \boldsymbol{\omega})$, we can simply keep one edge per parallelism class. We make that precise:

Definition 3.65. In a polytope P, two edges $\boldsymbol{uv}$ and $\boldsymbol{u'v'}$ are *parallel* when $\boldsymbol{v} - \boldsymbol{u}$ and $\boldsymbol{v'} - \boldsymbol{u'}$ are linearly dependent. The set of parallelism classes of edges P is denoted $\overline{E_{\boldsymbol{c}}}(\mathsf{P})$, and the number of classes $\overline{m}$.

Theorem 3.66. *For a linear program $(\mathsf{P}, \boldsymbol{c})$, fix a representative $\boldsymbol{f}_X$ for each class X of parallelism of edges in $\overline{E_{\boldsymbol{c}}}(\mathsf{P})$. Let $\rho : \mathbb{R}^m \to \mathbb{R}^{\overline{m}}$ be the projection that forgets all but the coordinates associated to $(\boldsymbol{f}_X)_{X \in \overline{E_{\boldsymbol{c}}}(\mathsf{P})}$. Then $\overline{\theta} := \rho \circ \theta : \mathbb{R}^d \to \mathbb{R}^{\overline{m}}$ is a linear injection.*

Moreover, $\overline{\theta}(\mathcal{N}(\mathcal{A}))$ is the intersection of $Im(\overline{\theta})$ with the pre-order cone of $\mathcal{B}_{\overline{m}}$ associated to the pre-order that $\preccurlyeq_{\mathcal{A}}$ induces on $\overline{E_{\boldsymbol{c}}}(\mathsf{P})$.

Proof. If $\boldsymbol{uv}$ and $\boldsymbol{u'v'}$ are parallel, then $\theta(\boldsymbol{\omega})_{\boldsymbol{uv}} = \frac{\langle \boldsymbol{\omega}, \boldsymbol{v}-\boldsymbol{u} \rangle}{\langle \boldsymbol{c}, \boldsymbol{v}-\boldsymbol{u} \rangle} = \frac{\langle \boldsymbol{\omega}, \boldsymbol{v'}-\boldsymbol{u'} \rangle}{\langle \boldsymbol{c}, \boldsymbol{v'}-\boldsymbol{u'} \rangle} = \theta(\boldsymbol{\omega})_{\boldsymbol{u'v'}}$. Consequently, if $\pi \circ \theta(\boldsymbol{\omega}) = \mathbf{0}$, then all coordinates of $\theta(\boldsymbol{\omega})$ are zero, and $\boldsymbol{\omega} = \mathbf{0}$ by injectivity of θ.

The above equality also implies that $\boldsymbol{uv} \simeq_{\mathcal{A}} \boldsymbol{u'v'}$ when $\boldsymbol{uv}$ and $\boldsymbol{u'v'}$ are parallel. So Lemma 3.51 ensures that the projection ρ sends the (triangulation of the) great cone associated to $\preccurlyeq_{\mathcal{A}}$ in $\mathcal{B}_m \cap \mathrm{Im}(\theta)$ onto the (triangulation of the) great cone associated to the quotient of $\preccurlyeq_{\mathcal{A}}$ on parallelism classes. □

We now use the power of these embeddings inside (sections of) braid fans to study the max-slope pivot polytopes of cubes, simplices and products of simplices.

3.3.1 Max-slope pivot polytopes of the cube and the simplex

Max-slope pivot polytope of a cube The standard cube $\square_d$ has been introduced in Section 1.2.2. Note that applying an affine transformation to P and $\boldsymbol{c}$ amounts to applying the same linear transformation to $\Pi(\mathsf{P}, \boldsymbol{c})$, by Theorem 3.6, so the case of the standard cube enlightens the case of all cubes with parallel edges, and gives a hint for the case of zonotopes (as projections of the standard cube). We are going to prove the following:

Theorem 3.67. *For any generic $\boldsymbol{c} \in \mathbb{R}^d$, the affine map $\overline{\theta}$ sends the max-slope pivot polytope $\Pi(\square_d, \boldsymbol{c})$ to (a polytope normally equivalent to) the permutahedron Π_d. Moreover, the normal cone $\mathcal{N}_{\mathcal{A}}$ of the vertex of $\Pi(\square_d, \boldsymbol{c})$ associated to $\mathcal{A}$ is sent to the pre-order cone of the pre-order $\preccurlyeq_{\mathcal{A}}$ induced on $\overline{E_{\boldsymbol{c}}}(\mathsf{P})$.*

This case was already studied in [BDLLS22, Example 4.2]: there, the authors prove that $\Pi(\square_d, \boldsymbol{c})$ is a permutahedron in the sense that it is the convex hull of the $d!$ points obtained from

applying the action of the permutation group $\mathcal{S}_d$ on a starting point. Though the computations are similar, we give here a different perspective.

Fix P to be the standard cube $\square_d$ of dimension d and $\boldsymbol{c} \in \mathbb{R}^d$ any generic objective function. By symmetry, we can suppose $c_1 < \cdots < c_d$. The vertices of the cube $\square_d$ identify with the subsets of $[d]$ through the characteristic vector: $\boldsymbol{e}_I := \sum_{i \in I} \boldsymbol{e}_i$ for a subset $I \subseteq [d]$, and $V(\square_d) = \{\boldsymbol{e}_I \ ; \ I \subseteq [d]\}$. The optimal vertex is $\boldsymbol{e}_{[d]}$. Moreover, the improving edges are of the for $\boldsymbol{e}_I \boldsymbol{e}_{I \cup \{i\}}$ for $i \notin I \subsetneq [d]$, and their parallelism class is given by $\boldsymbol{e}_i$, see Figure 52(Top Right).

Hence, there are $\overline{m} = d$ classes of parallelism of edges of $\square_d$. The linear map $\overline{\theta} : \mathbb{R}^d \to \mathbb{R}^{\overline{m}}$ injects the normal fan of $\Pi(\square_d, \boldsymbol{c})$ into the braid fan $\mathcal{B}_d$. As $\overline{m} = d$, $\overline{\theta}$ is surjective. This implies that $\Pi(\square_d, \boldsymbol{c})$ is a generalized permutahedron.

It remains to understand the fan $\overline{\theta}(\mathcal{N}_{\Pi(\mathsf{P},\boldsymbol{c})})$. Fix a multi-arborescence $\mathcal{A}$ on $\square_d$. Let σ be a surjection on $[d]$ that extends the pre-order induced by $\preccurlyeq_{\mathcal{A}}$ on $[d]$. Then for $i \neq j$, looking at $\mathcal{A}([d] \smallsetminus \{i,j\})$, one concludes that $\sigma(i) \leq \sigma(j)$ if and only if $[d] \smallsetminus \{i\} \in \mathcal{A}([d] \smallsetminus \{i,j\})$. Thus σ is fully determined by $\mathcal{A}$: the image $\overline{\theta}(\mathcal{N}(\mathcal{A}))$ is a cone C_σ for some surjection σ of $[d]$.

Example 3.68. In Figure 52(Top Right) is depicted the standard 3-dimensional cube $\square_3$, where each vertex is labelled by the corresponding set I (denoted without comma nor bracket). The objective function corresponds to the left-to-right orientation. The max-slope pivot polytope $\Pi(\square_3, \boldsymbol{c}) \simeq \Pi_3$ is the hexagon drawn on the left. Each vertex and each edge is labelled by a representation of the corresponding multi-arborescence $\mathcal{A}$, and the ordered partition whose associated surjection is the pre-order $\preccurlyeq_{\mathcal{A}}$ on $\overline{E}_{\boldsymbol{c}}(\square_3)$. For instance, the vertical edge on the right side corresponds to the multi-arborescence $\mathcal{A}$ with (using the notations of the figure) $\mathcal{A}(\varnothing) = \{1,3\}$, $\mathcal{A}(1) = \mathcal{A}(3) = \{13\}$, $\mathcal{A}(2) = \{12, 23\}$, $\mathcal{A}(13) = \mathcal{A}(12) = \mathcal{A}(23) = \{123\}$. Such multi-arborescence imposes that if $\boldsymbol{\omega} \in \mathbb{R}^3$ captures $\mathcal{A}$, then $\omega_2 < \omega_1 = \omega_3$.

Max-slope pivot polytope of a simplex As all simplices are affinely equivalent, for all linear program $(\mathsf{P}, \boldsymbol{c}')$ with P a simplex, Theorem 3.6 ensures that the max-slope pivot polytope $\Pi(\mathsf{P}, \boldsymbol{c}')$ is linearly equivalent to $\Pi(\Delta_d, \boldsymbol{c})$ where Δ_d is the standard simplex $\Delta_d = \operatorname{conv}\{\boldsymbol{e}_1, \dots \boldsymbol{e}_{d+1}\}$, and $c_1 < \cdots < c_{d+1}$. Hence, we are going to prove the following:

Theorem 3.69. *For any $\boldsymbol{c} \in \mathbb{R}^{d+1}$, the map ϑ sends the max-slope pivot polytope $\Pi(\Delta_d, \boldsymbol{c})$ to (a polytope normally equivalent to) Loday's associahedron Asso_d (that is a deformed permutahedron, see Section 1.2.4). Moreover, the normal cone $\mathcal{N}(\mathcal{A})$ of the vertex of $\Pi(\Delta_d, \boldsymbol{c})$ associated to $\mathcal{A}$ is sent by ϑ to the pre-order cone of the pre-order $\trianglelefteq_{\mathcal{A}}$ on $V(\mathsf{P}) \smallsetminus \{\boldsymbol{e}_{d+1}\}$.*

This case was already studied in [BDLLSon]: there the authors prove that $\Pi(\Delta_d, \boldsymbol{c})$ is combinatorially equivalent to Asso_d.

Contrarily to the case of the cube, there are $\binom{d}{2}$ classes of parallelisms of edges, so $\overline{\theta} : \mathbb{R}^d \to \mathbb{R}^{\binom{d}{2}}$ is injective but not surjective. However, $n - 1 = d$ (where n is the number of vertices of Δ_d), so for a multi-arborescence $\mathcal{A}$ on Δ_d, the map $\vartheta_{\mathcal{A}}$ is an endomorphism of $\mathbb{R}^d = \operatorname{aff}(\Delta_d)$.

For the simplex Δ_d, one can recover $\theta(\boldsymbol{\omega})$ from $\vartheta_{\mathcal{A}}(\boldsymbol{\omega})$ for all $\boldsymbol{\omega} \in \mathbb{R}^{d+1}$. Indeed, $\vartheta_{\mathcal{A}}$ is an automorphism because if $\vartheta_{\mathcal{A}}(\boldsymbol{\omega}) = \mathbf{0}$, then $\boldsymbol{\omega}$ is orthogonal to d different edges of Δ_d, so $\boldsymbol{\omega} = \mathbf{0}$ as d different edges of Δ_d spans $\mathbb{R}^d$. Thus, as $\vartheta_{\mathcal{A}} = \pi_{\mathcal{A}} \circ \theta$, the dimensions indicate that the map $\pi_{\mathcal{A}}$ is a bijection between $\operatorname{Im}(\theta)$ and $\operatorname{Im}(\vartheta_{\mathcal{A}})$. Consequently, ϑ is injective: if $\vartheta(\boldsymbol{\omega}) = \vartheta(\boldsymbol{\omega}')$, then $\theta(\boldsymbol{\omega}) = \theta(\boldsymbol{\omega}')$ by the previous argument, so $\boldsymbol{\omega} = \boldsymbol{\omega}'$ as θ is injective.

Therefore, ϑ is an injective piece-wise linear map from $\operatorname{aff}(\Delta_d)$ to $\mathbb{R}^d$: it is a bijection as their dimensions are equal[10]. Thus, $\Pi(\Delta_d, \boldsymbol{c})$ is combinatorially isomorphic to a generalized permutahedron. It remains to understand the normal fan of $\vartheta\big(\Pi(\Delta_d, \boldsymbol{c})\big)$.

To this end, it is enough to focus on the maximal cones of the fan $\vartheta\big(\Pi(\Delta_d, \boldsymbol{c})\big)$, *i.e.* to arborescences captured on Δ_d. Each such arborescence A can be seen as a map $A : [d+1] \to [d+1]$ with $A(i) > i$. For a coherent arborescence A on Δ_d, we have $A(i) = \min\big(\{j \ ; \ j > i \text{ and } j \preccurlyeq_A$

[10]Such a map induces a continuous injective application $\boldsymbol{\omega} \mapsto \frac{\vartheta(\boldsymbol{\omega})}{\|\vartheta(\boldsymbol{\omega})\|}$ of the d-dimensional sphere $\mathbb{S}^d$ to itself. If it were not surjective, it would induce an injection from $\mathbb{S}^d$ to $\mathbb{R}^d$ (which is homeomorphic to a sphere minus a point): Borsuk–Ulam's theorem ensures it does not exist. As $\vartheta(\lambda\boldsymbol{\omega}) = \lambda\vartheta(\boldsymbol{\omega})$, the map ϑ is bijective.

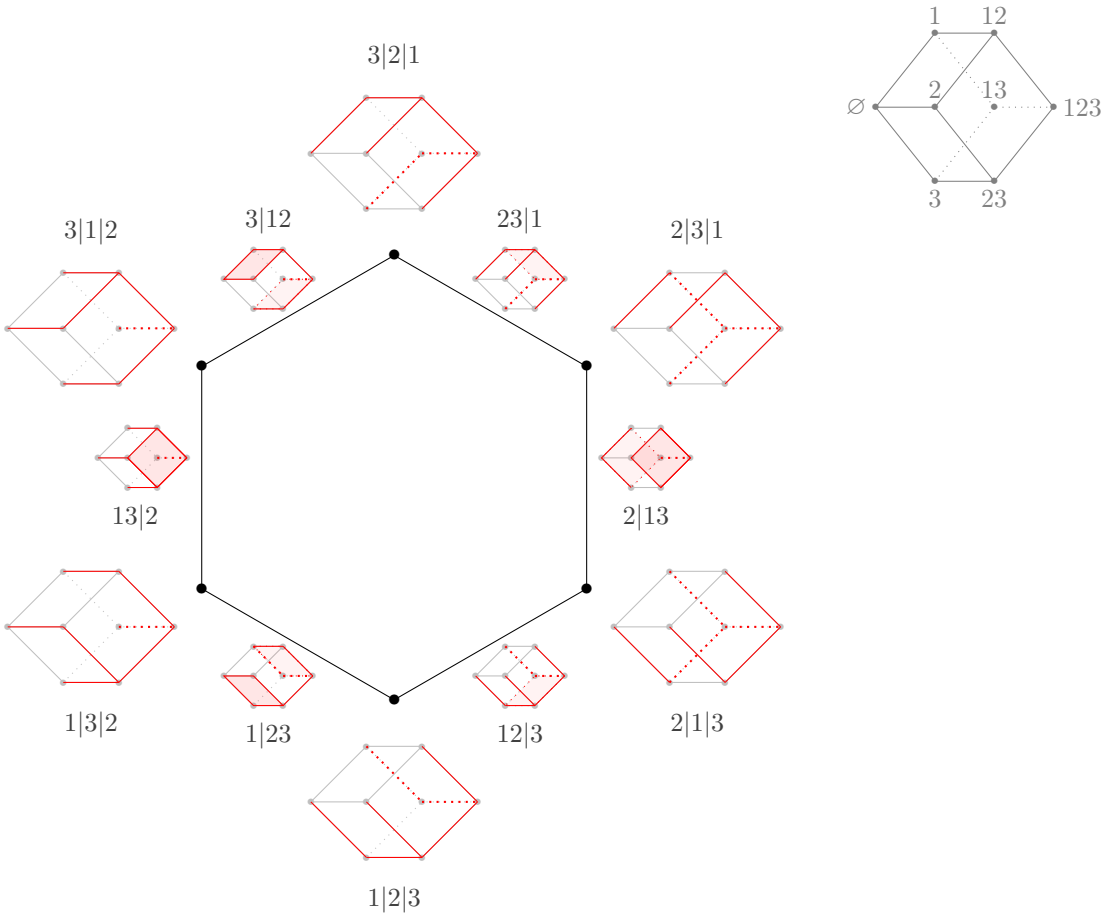

Figure 52: The max-slope pivot polytope of the cube $\square_3$ (the objective function is left to right). Each vertex is labelled by the corresponding multi-arborescence, and the surjection associated. For instance, the bottom vertex is associated with the arborescence $A^{\boldsymbol{\omega}}$ with $\omega_1 < \omega_2 < \omega_3$.

$i\} \cup \{d+1\}\big)$. Indeed, for a fixed i, on the one hand for all $i < j < A(i)$, Lemma 3.5 applied to the triangle (c_i, ω_i), (c_j, ω_j), $(c_{A(i)}, \omega_{A(i)})$ ensures that $i \preccurlyeq_A j$; and on the other hand, $A(i) \preccurlyeq_A i$ by Lemma 3.5 applied to the triangle (c_i, ω_i), $(c_{A(i)}, \omega_{A(i)})$, $(c_{A(A(i))}, \omega_{A(A(i))})$.

To a binary search tree T on $[d]$, one can associate the map $A_T : [d+1] \to [d+1]$ defined by $A_T(d+1) = d+1$ and $A_T(i) = \min\big(\{j \ ; \ j \notin T^i\} \cup \{d+1\}\big)$ where T^i is the sub-tree of root i in T. Fix a permutation σ and consider its binary search tree $T(\sigma)$, that is the binary search tree on $[d]$ in which i is inserted before j when $\sigma(i) < \sigma(j)$, see Section 1.2.4(paragraph Binary search trees). Then, $A_{T(\sigma)}$ is an arborescence such that σ extends $\trianglelefteq_{A_{T(\sigma)}}$. As ϑ is injective, $A_{T(\sigma)}$ is the unique arborescence with this property. Conversely, if two binary search trees T_1 and T_2 differ, then there exists i such that T_1^i and T_2^i differ, so $A_{T_1} \neq A_{T_2}$.

Hence, the map $T \mapsto A_T$ induces through ϑ a piece-wise linear isomorphism between $\mathcal{N}_{\Pi(\Delta_d, \boldsymbol{c})}$ and the coarsening of $\mathcal{B}_d$ defined by gluing C_σ and C_α when σ and α yield the same binary search tree, *i.e.* the sylvester fan. We have proven that $\Pi(\Delta_d, \boldsymbol{c})$ is piece-wise linearly equivalent to Loday's associahedron. Moreover, $\trianglelefteq_{\mathcal{A}}$ is precisely the pre-order associated to the normal cone $\vartheta(\mathcal{N}(\mathcal{A}))$.

Example 3.70. In Figure 53(Top Right) is depicted a 3-dimensional simplex Δ_3, where the vertices are labelled from 1 to 4 according to their scalar product against the (left-to-right oriented) objective function. The max-slope pivot polytope $\Pi(\Delta_3, \boldsymbol{c}) \simeq \mathsf{Asso}_3$ is drawn on the left. Each vertex is labelled three times. Firstly, by its non-crossing arborescence A (in the fashion of Sections 1.2.4 and 3.2). Secondly, by the pre-order $\trianglelefteq_A$ on $[3]$, figured as a binary search tree. Lastly, by the pre-order $\preccurlyeq_A$ on $E_{\boldsymbol{c}}(\Delta_3)$ (which has 6 edges, identified by the couple of vertices linked).

For instance, the rightmost vertex corresponds to the non-crossing arborescence A with $A(1) = 2$, $A(2) = A(3) = 4$, which adapted slope pre-order is defined by $2 \preccurlyeq_A 1$ and $2 \preccurlyeq_A 3$ (and no relation between 1 and 3), and utter slope pre-order can be read in increasing order from bottom to top on the rightmost part of Figure 53 (in red are the edges that A uses).

3.3.2 Max-slope pivot polytope of a product of simplices

The cartesian product of two polytopes $\mathsf{P} \subset \mathbb{R}^p$ and $\mathsf{Q} \subset \mathbb{R}^q$ is the polytope in $\mathbb{R}^{p+q} = \mathbb{R}^p \times \mathbb{R}^q$ defined as $\mathsf{P} \times \mathsf{Q} := \{(\boldsymbol{p}, \boldsymbol{q}) \ ; \ \boldsymbol{p} \in \mathsf{P}, \ \boldsymbol{q} \in \mathsf{Q}\}$. For two fixed polytopes P and Q and objective functions $\boldsymbol{c}_1 \in \mathbb{R}^p$ and $\boldsymbol{c}_2 \in \mathbb{R}^q$, suppose we know the max-slope pivot polytopes $\Pi(\mathsf{P}, \boldsymbol{c}_1)$ and $\Pi(\mathsf{Q}, \boldsymbol{c}_2)$: what can we say about the max-slope pivot polytope $\Pi(\mathsf{P} \times \mathsf{Q}, \boldsymbol{c})$ where $\boldsymbol{c} = (\boldsymbol{c}_1, \boldsymbol{c}_2)$?

We have already seen an instance of this problem: the standard cube $\square_d$ is the product of d segments $[0, 1]$, and its max-slope pivot polytope is the permutahedron. We will see that when P and Q are products of simplices, then $\Pi(\mathsf{P} \times \mathsf{Q}, \boldsymbol{c})$ is combinatorially isomorphic to the shuffle of $\Pi(\mathsf{P}, \boldsymbol{c}_1)$ and $\Pi(\mathsf{Q}, \boldsymbol{c}_2)$ as defined in [CP22, Section 2]. We will not be able to fully describe the general case, but some interesting general properties will spring from the discussion that follows.

Definition 3.71. ([CP22, Definition 75]). The *shuffle product* of two generalized permutahedra $\mathsf{P} \subset \mathbb{R}^p$ and $\mathsf{Q} \subset \mathbb{R}^q$ is the polytope $\mathsf{P} \star \mathsf{Q} \subset \mathbb{R}^{p+q}$ defined by:

$$\mathsf{P} \star \mathsf{Q} = \mathsf{P} \times \mathsf{Q} + \sum_{i \in [p], \ j \in [q]} [\boldsymbol{e}_i, \boldsymbol{e}_{p+j}]$$

Definition 3.72. Given two pre-orders $\leq$ on a set E and $\preccurlyeq$ on a set F, a pre-order $\trianglelefteq$ on $E \sqcup F$ is *shuffle of $\leq$ and $\preccurlyeq$* when the four following conditions hold:

- for all $e, e' \in E$, if $e \leq e'$ then $e \trianglelefteq e'$;
- for all $f, f' \in F$, if $f \preccurlyeq f'$, then $f \trianglelefteq f'$;
- for all $e \in E, f \in F$, either $e \trianglelefteq f$ or $f \trianglelefteq e$;
- $\trianglelefteq$ is the closure relation of the above (that is, for all $e, e' \in E$, if $e \trianglelefteq e'$, then either $e \leq e'$ or there exists $f \in F$ such that $e \trianglelefteq f \trianglelefteq e'$, and conversely for $f, f' \in F$).

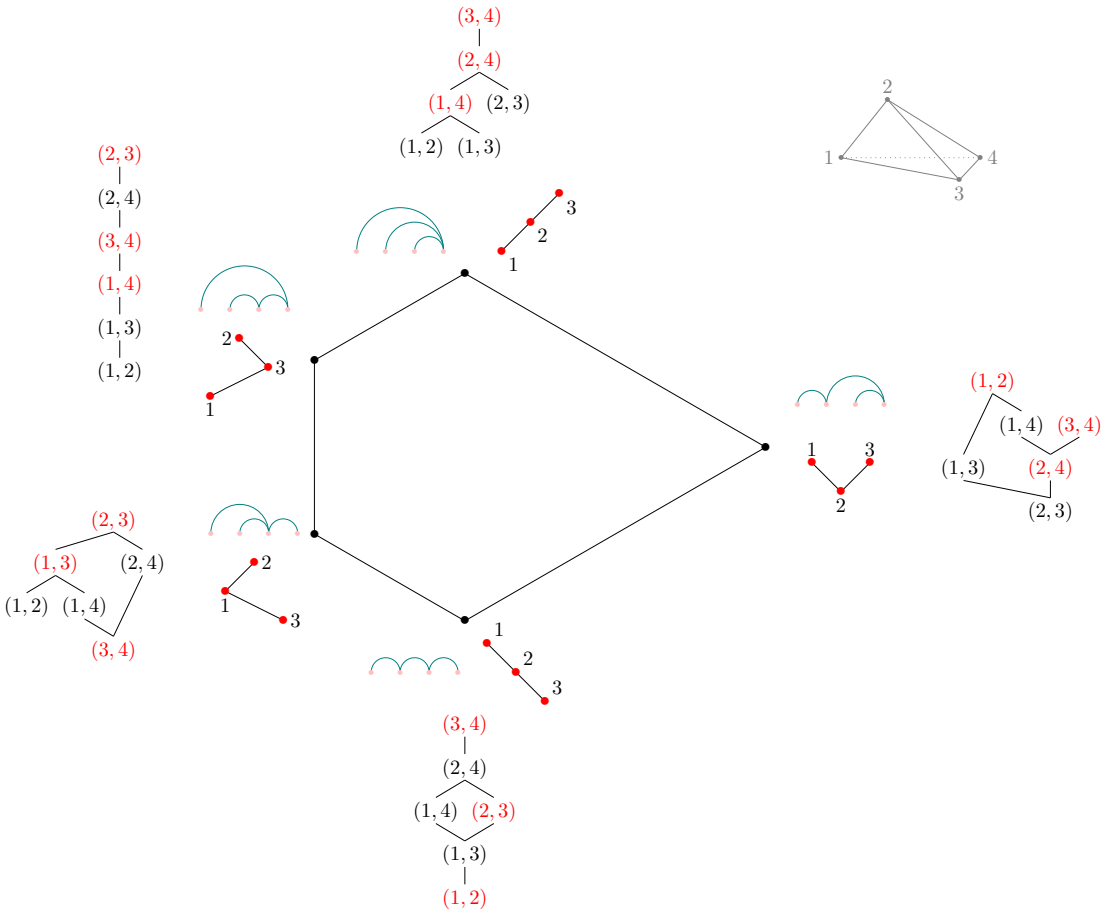

Figure 53: The max-slope pivot polytope of the simplex Δ_3. Each vertex is labelled by the corresponding (coherent) non-crossing arborescence A, the binary search tree T with $A = A_T$, and the pre-order $\preccurlyeq_A$ on the edges of Δ_3.

Recall that each cone of the normal fan of a deformed permutahedron is a pre-order cone.

Proposition 3.73. ([CP22, Proposition 79]). *For* P *and* Q *two deformed permutahedra, the normal fan of* $\mathsf{P} \star \mathsf{Q}$ *is precisely the set of pre-order cones* $\mathsf{C}_{\trianglelefteq}$ *where* $\trianglelefteq$ *runs over all shuffles between a pre-order* $\leq$ *corresponding to a normal cone of* P *and a pre-order* $\preccurlyeq$ *corresponding to a normal cone of* Q.

We are going to prove the following:

Theorem 3.74. *If* P *is (isomorphic to) a product of simplices* $\Delta_{d_1} \times \cdots \times \Delta_{d_r}$ *with* $d = \sum_{i=1}^{r} d_i$, *then for any generic objective function* $\boldsymbol{c}$, *there exists a piece-wise linear map* $\overline{\vartheta}$ *(explicitly defined hereafter) that sends the max-slope pivot polytope* $\Pi(\mathsf{P}, \boldsymbol{c})$, *to (a polytope normally equivalent to) the shuffle product* $\mathsf{Asso}_{d_1} \star \cdots \star \mathsf{Asso}_{d_r}$.

Moreover, the normal cone $\mathcal{N}(\mathcal{A})$ *of the vertex of* $\Pi(\mathsf{P}, \boldsymbol{c})$ *associated to* $\mathcal{A}$ *is sent by* $\overline{\vartheta}$ *to the pre-order cone of the pre-order that* $\trianglelefteq_{\mathcal{A}}$ *induces on* $\prod_{i=1}^{r} V(\Delta_{d_i}) \smallsetminus \{\boldsymbol{e}_{d_i+1}\}$.

Proof. Although the notations can feel heavy, we are simply going to work with (piece-wise) linear functions, and analyze which pre-orders are associated to which cones.

We first focus on classes of parallelism on $\mathsf{P} \times \mathsf{Q}$. Fix polytopes $\mathsf{P} \subset \mathbb{R}^p$ and $\mathsf{Q} \subset \mathbb{R}^q$ with generic objective functions $\boldsymbol{c}_1 \in \mathbb{R}^p$ and $\boldsymbol{c}_2 \in \mathbb{R}^q$. We denote $\boldsymbol{p}_{\mathrm{opt}}$ the optimal vertex of P with respect to $\boldsymbol{c}_1$, and $\boldsymbol{q}_{\mathrm{opt}}$ the optimal vertex of Q with respect to $\boldsymbol{c}_2$. Take a coherent multi-arborescence $\mathcal{A}$ on $\mathsf{P} \times \mathsf{Q}$ captured by $\boldsymbol{\omega} = (\boldsymbol{\omega}_1, \boldsymbol{\omega}_2) \in \mathbb{R}^p \times \mathbb{R}^q$. Remark that $\mathcal{A}$ induces a coherent multi-arborescence $\mathcal{A}_{\mathsf{P}}$ on P and a coherent multi-arborescence $\mathcal{A}_{\mathsf{Q}}$ on Q defined as follows: $\mathcal{A}_{\mathsf{P}}(\boldsymbol{u}) \times \{\boldsymbol{q}_{\mathrm{opt}}\} = \mathcal{A}((\boldsymbol{u}, \boldsymbol{q}_{\mathrm{opt}}))$ and $\{\boldsymbol{p}_{\mathrm{opt}}\} \times \mathcal{A}_{\mathsf{Q}}(\boldsymbol{v}) = \mathcal{A}((\boldsymbol{p}_{\mathrm{opt}}, \boldsymbol{v}))$. Manifestly, these multi-arborescences are coherent as they are captured by $\boldsymbol{\omega}_1$ and $\boldsymbol{\omega}_2$ respectively.

Then note that for any $\boldsymbol{p}, \boldsymbol{p}' \in V(\mathsf{P})$ and $\boldsymbol{q} \in V(\mathsf{Q})$, the edges $(\boldsymbol{p}, \boldsymbol{q})(\boldsymbol{p}', \boldsymbol{q})$ and $(\boldsymbol{p}, \boldsymbol{q}_{\mathrm{opt}})(\boldsymbol{p}', \boldsymbol{q}_{\mathrm{opt}})$ are parallel (and respectively for Q). Hence, there are three possibilities: either $\mathcal{A}((\boldsymbol{p}, \boldsymbol{q})) = \mathcal{A}_{\mathsf{P}}(\boldsymbol{p}) \times \{\boldsymbol{q}\}$, or $\mathcal{A}((\boldsymbol{p}, \boldsymbol{q})) = \{\boldsymbol{p}\} \times \mathcal{A}_{\mathsf{Q}}(\boldsymbol{q})$, or $\mathcal{A}((\boldsymbol{p}, \boldsymbol{q})) = \mathcal{A}_{\mathsf{P}}(\boldsymbol{p}) \times \mathcal{A}_{\mathsf{Q}}(\boldsymbol{q})$, depending on the (in)equality between $\tau_{\boldsymbol{\omega}_1}(\mathcal{A}_{\mathsf{P}}(\boldsymbol{p}))$ and $\tau_{\boldsymbol{\omega}_2}(\mathcal{A}_{\mathsf{Q}}(\boldsymbol{q}))$. This allows us to associate to $\mathcal{A}$ a pre-order $\trianglelefteq_{\mathcal{A},\|}$ on $\big(V(\mathsf{P}) \smallsetminus \{\boldsymbol{p}_{\mathrm{opt}}\}\big) \sqcup \big(V(\mathsf{Q}) \smallsetminus \{\boldsymbol{q}_{\mathrm{opt}}\}\big)$ defined by (the closure of):

$$\begin{cases} \boldsymbol{p} \trianglelefteq_{\mathcal{A},\|} \boldsymbol{p}' & \text{if} \quad (\boldsymbol{p}, \boldsymbol{q}_{\mathrm{opt}}) \trianglelefteq_{\mathcal{A}} (\boldsymbol{p}', \boldsymbol{q}_{\mathrm{opt}}) \\ \boldsymbol{q} \trianglelefteq_{\mathcal{A},\|} \boldsymbol{q}' & \text{if} \quad (\boldsymbol{p}_{\mathrm{opt}}, \boldsymbol{q}) \trianglelefteq_{\mathcal{A}} (\boldsymbol{p}_{\mathrm{opt}}, \boldsymbol{q}') \\ \boldsymbol{p} \triangleleft_{\mathcal{A},\|} \boldsymbol{q} & \text{if} \quad \mathcal{A}((\boldsymbol{p}, \boldsymbol{q})) = \{\boldsymbol{p}\} \times \mathcal{A}_{\mathsf{Q}}(\boldsymbol{q}) \\ \boldsymbol{q} \triangleleft_{\mathcal{A},\|} \boldsymbol{p} & \text{if} \quad \mathcal{A}((\boldsymbol{p}, \boldsymbol{q})) = \mathcal{A}_{\mathsf{P}}(\boldsymbol{p}) \times \{\boldsymbol{q}\} \\ \boldsymbol{p} \simeq_{\mathcal{A},\|} \boldsymbol{q} & \text{if} \quad \mathcal{A}((\boldsymbol{p}, \boldsymbol{q})) = \mathcal{A}_{\mathsf{P}}(\boldsymbol{p}) \times \mathcal{A}_{\mathsf{Q}}(\boldsymbol{q}) \end{cases}$$

The pre-order $\trianglelefteq_{\mathcal{A}}$ can be retrieved from the knowledge of $\trianglelefteq_{\mathcal{A},\|}$, as we only have quotiented (certain) equivalence classes: $(\boldsymbol{p}, \boldsymbol{q}) \simeq_{\mathcal{A}} (\boldsymbol{p}, \boldsymbol{q}_{\mathrm{opt}})$ when $\boldsymbol{q} \trianglelefteq_{\mathcal{A},\|} \boldsymbol{p}$; and $(\boldsymbol{p}, \boldsymbol{q}) \simeq_{\mathcal{A}} (\boldsymbol{p}_{\mathrm{opt}}, \boldsymbol{q})$ when $\boldsymbol{p} \trianglelefteq_{\mathcal{A},\|} \boldsymbol{q}$.

Consequently, when $\mathsf{P} = \Delta_{d_1} \times \cdots \times \Delta_{d_r}$ (where $\sum_i d_i = p = \dim(\mathsf{P})$) is a product of simplices, the above process allows us to associate injectively a pre-order $\trianglelefteq_{\mathcal{A},\|}$ on $\bigsqcup_i V(\Delta_{d_i}) \smallsetminus \{\boldsymbol{e}_{d_i+1}\}$ to the pre-order $\trianglelefteq_{\mathcal{A}}$, for each multi-arborescence $\mathcal{A}$ on P.

Now, we prove by induction on the number of factors that when P is a product of simplices $\Delta_{d_1} \times \cdots \times \Delta_{d_r}$, then there exists a piece-wise linear (continuous) bijection $\overline{\vartheta}_{\mathsf{P}} : \mathbb{R}^p \to \mathbb{R}^p$ that embeds $\mathcal{N}_{\Pi(\mathsf{P}, \boldsymbol{c}_1)}$ into $\mathcal{B}_p$ where $\overline{\vartheta}_{\mathsf{P}}(\mathcal{N}(\mathcal{A}_{\mathsf{P}}))$ is the pre-order cone $\mathsf{C}_{\trianglelefteq_{\mathcal{A}_{\mathsf{P}},\|}}$. Fix two products of simplices P and Q and suppose the statement holds, denoting $\overline{\vartheta}_{\mathsf{P}} : \mathbb{R}^p \to \mathbb{R}^p$ for P and $\overline{\vartheta}_{\mathsf{Q}} : \mathbb{R}^q \to \mathbb{R}^q$ for Q. Then define $\overline{\vartheta} : \mathbb{R}^{p+q} \to \mathbb{R}^{p+q}$ by setting $\overline{\vartheta}\big((\boldsymbol{\omega}_{\mathsf{P}}, \boldsymbol{\omega}_{\mathsf{Q}})\big) = \big(\overline{\vartheta}_{\mathsf{P}}(\boldsymbol{\omega}_{\mathsf{P}}),\ \overline{\vartheta}_{\mathsf{Q}}(\boldsymbol{\omega}_{\mathsf{Q}})\big)$. The application $\overline{\vartheta}$ is a piece-wise linear (continuous) bijection as $\overline{\vartheta}_{\mathsf{P}}$ and $\overline{\vartheta}_{\mathsf{Q}}$ are. It embeds $\overline{\vartheta}(\mathcal{N}_{\Pi(\mathsf{P} \times \mathsf{Q}, \boldsymbol{c})})$ into the braid fan $\mathcal{B}_{p+q}$. Moreover, for a multi-arborescence $\mathcal{A}$ on $\mathsf{P} \times \mathsf{Q}$, if σ is a surjection of $[p] \sqcup [q]$ that extends $\trianglelefteq_{\mathcal{A},\|}$, the definition of this pre-order ensures that if $\boldsymbol{\omega} \in \mathbb{R}^{p+q}$ satisfies $\overline{\vartheta}(\boldsymbol{\omega}) \in \mathsf{C}_{\sigma}$, then $\boldsymbol{\omega}$ captures $\mathcal{A}$. As $\overline{\vartheta}$ is bijective, the cone $\overline{\vartheta}(\mathcal{N}(\mathcal{A}))$ is the union of cones C_{σ} for σ that extends $\trianglelefteq_{\mathcal{A},\|}$. As the statement holds for any simplex by Theorem 3.69, the induction follows.

We have proven that $\Pi(\mathsf{P}\times\mathsf{Q},\boldsymbol{c})$ is a generalized permutahedron, as $\overline{\vartheta}$ sends bijectively the normal fan of $\Pi(\mathsf{P}\times\mathsf{Q},\boldsymbol{c})$ on a fan coarsening $\mathcal{B}_{p+q}$. It remains to understand this coarsening. As $\mathsf{P}=\Delta_{d_1}\times\dots\Delta_{d_r}$, we denote $\overline{V}(\mathsf{P}):=\bigsqcup_i V(\Delta_{d_i})\smallsetminus\{\boldsymbol{e}_{d_i+1}\}$. Fix a multi-arborescence $\mathcal{A}$ on $\mathsf{P}\times\mathsf{Q}$ and defined as before: $\mathcal{A}_{\mathsf{P}}(\boldsymbol{u})\times\{\boldsymbol{q}_{\mathrm{opt}}\}=\mathcal{A}((\boldsymbol{u},\boldsymbol{q}_{\mathrm{opt}}))$ and $\{\boldsymbol{p}_{\mathrm{opt}}\}\times\mathcal{A}_{\mathsf{Q}}(\boldsymbol{v})=\mathcal{A}((\boldsymbol{p}_{\mathrm{opt}},\boldsymbol{v}))$. Associate to $\mathcal{A}$ the pre-order $\trianglelefteq$ on $\overline{V}(\mathsf{P})\sqcup\overline{V}(\mathsf{Q})$ that is the shuffle of $\trianglelefteq_{\mathcal{A}_{\mathsf{P}},\|}$ and $\trianglelefteq_{\mathcal{A}_{\mathsf{Q}},\|}$ defined as the transitive closure of the following relations:

$$\begin{cases}\boldsymbol{p}\trianglelefteq\boldsymbol{p}' & \text{if}\quad \boldsymbol{p}\trianglelefteq_{\mathcal{A}_{\mathsf{P}},\|}\boldsymbol{p}'\\ \boldsymbol{q}\trianglelefteq\boldsymbol{q}' & \text{if}\quad \boldsymbol{q}\trianglelefteq_{\mathcal{A}_{\mathsf{Q}},\|}\boldsymbol{q}'\\ \boldsymbol{p}\trianglelefteq\boldsymbol{q} & \text{if}\quad \{\boldsymbol{p}\}\times\mathcal{A}_{\mathsf{Q}}(\boldsymbol{q})\subseteq\mathcal{A}((\boldsymbol{p},\boldsymbol{q}))\\ \boldsymbol{q}\trianglelefteq\boldsymbol{p} & \text{if}\quad \mathcal{A}_{\mathsf{P}}(\boldsymbol{q})\times\{\boldsymbol{q}\}\subseteq\mathcal{A}((\boldsymbol{p},\boldsymbol{q}))\end{cases}$$

If a surjection σ of $[p]\sqcup[q]$ extends this shuffle pre-order $\trianglelefteq$, then $\mathsf{C}_\sigma\subseteq\overline{\vartheta}(\mathcal{N}(\mathcal{A}))$. Indeed, as $\overline{\vartheta}$ is bijective, take $\boldsymbol{x}\in\mathsf{C}_\sigma$ and $\boldsymbol{\omega}=(\boldsymbol{\omega}_1,\boldsymbol{\omega}_2)$ with $\overline{\vartheta}(\boldsymbol{\omega})=\boldsymbol{x}$, then $\boldsymbol{\omega}_1$ captures $\mathcal{A}_{\mathsf{P}}$ on P, and $\boldsymbol{\omega}_2$ captures $\mathcal{A}_{\mathsf{Q}}$ on Q, by definitions of $\overline{\vartheta}_{\mathsf{P}}$ and $\overline{\vartheta}_{\mathsf{Q}}$. Furthermore, $\boldsymbol{p}\trianglelefteq\boldsymbol{q}$ if and only if $\{\boldsymbol{p}\}\times\mathcal{A}_{\mathsf{Q}}(\boldsymbol{q})\subseteq\mathcal{A}((\boldsymbol{p},\boldsymbol{q}))$, so $\boldsymbol{x}\in\overline{\vartheta}(\mathcal{N}(\mathcal{A}))$ as σ extends $\trianglelefteq$. Conversely, if $\boldsymbol{x}=\overline{\vartheta}((\boldsymbol{\omega}_1,\boldsymbol{\omega}_2))\in\mathsf{C}_\alpha$ for α that does not extend $\trianglelefteq$, then there exists $\boldsymbol{r},\boldsymbol{r}'\in\overline{V}(\mathsf{P})\sqcup\overline{V}(\mathsf{Q})$ such that $\boldsymbol{r}\trianglelefteq\boldsymbol{r}'$ but $\alpha(\boldsymbol{r})>\alpha(\boldsymbol{r}')$. If $\boldsymbol{r},\boldsymbol{r}'\in\overline{V}(\mathsf{P})$, then the definition of $\leq_{\mathcal{A}_{\mathsf{P}},\|}$ ensures that $\boldsymbol{\omega}_1$ does not capture P, and idem if $\boldsymbol{r},\boldsymbol{r}'\in\overline{V}(\mathsf{Q})$. And if $\boldsymbol{r}\in\overline{V}(\mathsf{P})$ while $\boldsymbol{r}'\in\overline{V}(\mathsf{Q})$, then $\tau_{\boldsymbol{\omega}_1}(\mathcal{A}_{\mathsf{P}}(\boldsymbol{p}))>\tau_{\boldsymbol{\omega}_2}(\mathcal{A}_{\mathsf{Q}}(\boldsymbol{q}))$, so $\{\boldsymbol{p}\}\times\mathcal{A}_{\mathsf{Q}}(\boldsymbol{q})\not\subseteq\mathcal{A}((\boldsymbol{p},\boldsymbol{q}))$. In any case, $\boldsymbol{x}\notin\overline{\vartheta}(\mathcal{N}(\mathcal{A}))$.

We have proven that $\mathsf{C}_\sigma\subseteq\overline{\vartheta}(\mathcal{N}(\mathcal{A}))$ if and only if σ extends the shuffle $\trianglelefteq_{\mathcal{A}_{\mathsf{P}},\|}$ and $\trianglelefteq_{\mathcal{A}_{\mathsf{Q}},\|}$ that $\trianglelefteq$ defines. Moreover, as Proposition 3.73 ensures that the shuffle product $\Pi(\mathsf{P},\boldsymbol{c}_1)\star\Pi(\mathsf{Q},\boldsymbol{c}_2)$ is realizable, we obtain that $\overline{\vartheta}(\mathcal{N}(\mathcal{A}))$ is the pre-order cone $\mathsf{C}_{\trianglelefteq}$. Together with Theorem 3.69, this proves the claimed theorem. □

Example 3.75. Theorem 3.74 grants access to several examples, studied in details in [CP22, Sections 3 & 4]. We briefly review the most prominent, and the combinatorial families they are associated to.

Let $\mathsf{P}=\Delta_{d_1}\times\dots\Delta_{d_r}$ be a product of simplices, then:

(a) When $r=1$, $\mathsf{P}=\Delta_d$ is a simplex, and $\Pi(\Delta_d,\boldsymbol{c})$ is an associahedron Asso_d (see Theorem 3.69). Its vertices correspond to binary trees.

(b) When $d_i=1$ for all i, $\mathsf{P}=\square_d$ is the standard cube and $\Pi(\square_d,\boldsymbol{c})$ is a permutahedron Π_d (see Theorem 3.67). Its vertices correspond to permutations.

(c) When $r=2$, $d_1=1$ and $d_2=n$, then $\mathsf{P}=\Delta_1\times\Delta_n$ is a prism over a simplex, and $\Pi(\Delta_1\times\Delta_n,\boldsymbol{c})$ is the *multiplihedron* (see [Sta70, For08]). More generally, when $r=m+1$, $d_1=\dots=d_m=1$ and $d_{m+1}=n$, then $\mathsf{P}=\square_m\times\Delta_n$ is the product of a cube and a simplex, and $\Pi(\square_m\times\Delta_n,\boldsymbol{c})$ is the *(m,n)-multiplihedron* as defined in [CP22, Section 3.2]. Its vertices correspond to painted trees.

(d) When $r=2$, $d_1=n$ and $d_2=m$, then $\mathsf{P}=\Delta_m\times\Delta_n$ is the product of two simplices, and $\Pi(\Delta_m\times\Delta_n,\boldsymbol{c})$ is the *(m,n)-constrainahedron* (see [Bot19, Pol21] and [CP22, Section 4]). Its vertices correspond to cotrees.

Example 3.76. For any P and Q, each coherent multi-arborescence $\mathcal{A}$ on $\mathsf{P}\times\mathsf{Q}$ is associated with a pre-order $\leq$ on $\big(V(\mathsf{P})\smallsetminus\{\boldsymbol{p}_{\mathrm{opt}}\}\big)\sqcup\big(V(\mathsf{Q})\smallsetminus\{\boldsymbol{q}_{\mathrm{opt}}\}\big)$ that is a shuffle between some pre-orders $\leq_{\mathcal{A}_{\mathsf{P}}}$ and $\leq_{\mathcal{A}_{\mathsf{Q}}}$ for $\mathcal{A}_{\mathsf{P}}$ and $\mathcal{A}_{\mathsf{Q}}$ as defined before. The map $\mathcal{A}\mapsto\leq$ is injective, as we have seen that the knowledge of all comparisons given by $\leq$ allows to recover the multi-arborescences. Nevertheless, $\trianglelefteq_{\mathcal{A}}$ is not necessarily isomorphic to $\leq$, but only extends it[11].

Moreover, in the general case when P or Q is not a product of simplicies, not all shuffles between coherent pre-orders on P and on Q are associated to a coherent pre-order on $\mathsf{P}\times\mathsf{Q}$ by this construction. To illustrate this fact, consider the following example. Fix $\boldsymbol{v}_1=\begin{pmatrix}0\\0\end{pmatrix}$, $\boldsymbol{v}_2=\begin{pmatrix}1\\0\end{pmatrix}$, $\boldsymbol{v}_3=\begin{pmatrix}0\\1\end{pmatrix}$ and $\boldsymbol{v}_4=\begin{pmatrix}2\\1\end{pmatrix}$ and let $\mathsf{P}=\operatorname{conv}\{\boldsymbol{v}_1,\boldsymbol{v}_2,\boldsymbol{v}_3,\boldsymbol{v}_4\}$ with $\boldsymbol{c}=(1,1)$, see

[11] The author sees no proof of isomorphism in general but is still trying to find a counter-example.

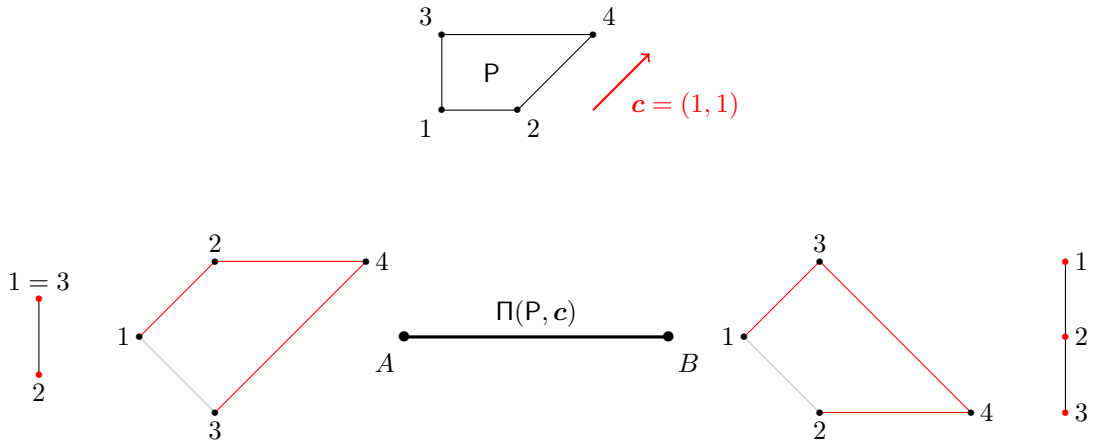

Figure 54: A non-standard square P (Top) and its max-slope pivot polytope (Bottom), labelled by its corresponding (coherent) arborescence A and B, together with their its adapted slope pre-orders $\trianglelefteq_A$ and $\trianglelefteq_B$.

Figure 54(Top). Note that the edges $\boldsymbol{v}_1\boldsymbol{v}_2$ and $\boldsymbol{v}_3\boldsymbol{v}_4$ are parallel, while $\boldsymbol{v}_1\boldsymbol{v}_3$ and $\boldsymbol{v}_2\boldsymbol{v}_4$ are not. As P is 2-dimensional, $\Pi(\mathsf{P}, \boldsymbol{c})$ is 1-dimensional and has two vertices. With the help of a computer, one can determine that the first vertex is associated with the arborescence (for convenience, we identify $\boldsymbol{v}_i$ with $i \in [4]$) A with $A(1) = 2$, $A(2) = 4$ and $A(3) = 4$, giving rise to the pre-order $\leq_A$ defined by $2 <_A 1 =_A 3$, see Figure 54(Bottom Left). The second vertex is associated with the arborescence B with $B(1) = 3$, $B(2) = 4$ and $B(3) = 4$, giving rise to the pre-order $\leq_B$ defined by $1 <_B 3 <_B 2$, see Figure 54(Bottom Right).

Define $\overline{\theta} : \mathbb{R}^2 \to \mathbb{R}^3$ by $\overline{\theta}(\boldsymbol{\omega}) = \big(\tau_{\boldsymbol{\omega}}(\boldsymbol{v}_1\boldsymbol{v}_2),\ \tau_{\boldsymbol{\omega}}(\boldsymbol{v}_2\boldsymbol{v}_4),\ \tau_{\boldsymbol{\omega}}(\boldsymbol{v}_1\boldsymbol{v}_3)\big)$. As we observe that $\boldsymbol{v}_4 - \boldsymbol{v}_2 = (\boldsymbol{v}_3 - \boldsymbol{v}_1) + (\boldsymbol{v}_2 - \boldsymbol{v}_1)$, one has that $\mathrm{Im}(\overline{\theta}) = \big\{(x, y, z) \in \mathbb{R}^3 \ ;\ z = \frac{x+y}{2}\big\}$, so in particular, for all $\boldsymbol{\omega} \in \mathbb{R}^2$, the second coordinate of $\overline{\theta}(\boldsymbol{\omega})$ is always in-between the two others: the only pre-order cones of $\mathcal{B}_3$ that intersects $\mathrm{Im}(\overline{\theta})$ are the ones associated with the pre-order $1 < 2 < 3$ (corresponding the arborescence B) and $3 < 2 < 1$ (corresponding to the arborescence A).

Now, we consider $\mathsf{P}^2 = \mathsf{P} \times \mathsf{P}$. Our computer experiment indicates that $\Pi(\mathsf{P}^2, (\boldsymbol{c}, \boldsymbol{c}))$ has 44 vertices. But there are 46 possible shuffles between $\leq_A$ and $\leq_B$, indeed:

$$\binom{2+2}{2} + \binom{2+3}{2} + \binom{3+2}{3} + \binom{3+3}{3} = 6 + 10 + 10 + 20 = 46$$

In the product P^2, we denote (i, j) for $i, j \in \{1, 2, 3, 4\}$ the vertex $(\boldsymbol{v}_i, \boldsymbol{v}_j)$. The couple $(4, 4)$ represents the optimal vertex $(\boldsymbol{v}_4, \boldsymbol{v}_4)$, and the support of the shuffles of A and B is $\{(i, 4)\}_{1 \leq i \leq 3} \sqcup \{(4, i)\}_{1 \leq i \leq 3}$. Thanks to our computer experiment, we can identify the two shuffles of A and B that do not correspond to vertices of $\Pi(\mathsf{P}^2, \boldsymbol{c})$: they are $(3, 4) < (4, 3) < (4, 2) < (2, 4) < (1, 4) < (4, 1)$ and its symmetric.

3.3.3 Perspectives and open questions

Computational remarks First of all, as for the other sections, I have implemented with Sage the main objects of the present section. To begin with, the computation of max-slope pivot polytopes is done as a sum of sections, see Figure 28. For a d-dimensional polytope P with $n = |V(\mathsf{P})|$, although this method seems efficient (as it does not require running through all possible arborescences and identify the coherent ones), it needs to construct $n - 1$ polytopes of dimension $d - 1$ and compute their Minkowski sum: even the max-slope pivot polytope of the product of two pentagons ($d = 4$

and $n = 25$) takes time. A better implementation of max-slope pivot polytopes would thus be important for more involved computations.

Besides, I have also implemented the computations of the utter and adapted slope pre-orders $\preccurlyeq_{\mathcal{A}}$ and $\trianglelefteq_{\mathcal{A}}$: for a linear program $(\mathsf{P}, \boldsymbol{c})$, my implementation can list the coherent arborescences together with their pre-orders, and determine (the coordinates and normal cone of) the associated vertex in $\Pi(\mathsf{P}, \boldsymbol{c})$.

Assets and limits of the current approach, open questions The above map $\overline{\vartheta}$ is very suitable for the study of product of simplices, but seems not exactly fit for products of other polytopes. Indeed, to replicate the proof of Theorem 3.69, the key point would be to decompose a polytope P as a product $\mathsf{P} = \mathsf{P}_1 \times \cdots \times \mathsf{P}_r$ (where each P_i can not be written as a product), and to have each P_i endowed with a piece-wise linear bijection $\vartheta_i : \mathbb{R}^d \to \mathbb{R}^{n-1}$. But this would mean that $n - 1 = d$, so P_i is a simplex.

Nevertheless, multiple ideas are to be retrieved from the study lead previously.

First, Conjecture 3.64 indicates that numerous links between the realm of max-slope pivot polytopes and generalized permutahedra are to be discovered. Especially, it advocates for a new way of thinking of slope comparisons, as comparisons between coordinates of a linear transformation.

Furthermore, this framework is efficient for quotienting parallelism of edges. For instance, all generalized permutahedra $\mathsf{P} \subset \mathbb{R}^n$ have (at most) $\binom{n}{2}$ classes of edge parallelism[12], indicating that all generalized permutahedra have *morally* the same complexity in terms of combinatorial behavior of the max-slope pivot rule (except for cubes, simplices, etc, which are simpler). It would be interesting to study the impact of other symmetries, for example by studying polytopes with central symmetry such as zonotopes, or classes of polytopes closed by taking faces such as hypersimplices.

Besides, the above Example 3.76 points out that, in general, the max-slope pivot polytope of a product $\mathsf{P} \times \mathsf{Q}$, even though not being the shuffle product of the max-slope pivot polytope of P and Q, is not far from being so. This shuffle product is not in general well-defined (as a polytope), as shuffle product is only defined for generalized permutahedra, but it is defined as a poset: it is the poset consisting of all shuffles between pre-orders of coherent multi-arborescences on P and pre-orders of coherent multi-arborescences on Q. The face lattice of $\Pi(\mathsf{P} \times \mathsf{Q}, (\boldsymbol{c}_1, \boldsymbol{c}_2))$ injects in this poset, and one can wonder how distinct the two can be.

Last but not least, an important open problem is to determine for which linear program $(\mathsf{P}, \boldsymbol{c})$ does the max-slope pivot polytope $\Pi(\mathsf{P}, \boldsymbol{c})$ is (combinatorially or piece-wise linearly isomorphic to) a generalized permutahedron. We have proven it happens for products of simplices. On the opposite, for cyclic polytopes it can not be the case in general, as the 2-dimensional $\Pi(\mathsf{Cyc}_3(\boldsymbol{t}), \boldsymbol{e}_1)$ and $\mathsf{Asso}_d(\boldsymbol{t})$ already have too many vertices, see Section 3.2 and Corollaries 3.37 and 3.49. However, the problem remains open, and finding a polytope P such that its max-slope pivot polytope is a generalized permutahedron would grant a powerful tool to study the behavior of the simplex method on P, while providing a very interesting example.

[12] As generalized permutahedra are (edge-)deformations of Π_n, all their edges are parallel to edges of Π_n, that is to say to $\boldsymbol{e}_j - \boldsymbol{e}_i$ for some $i, j \in [n]$ with $i \neq j$, limiting the number of classes of parallelism to at most $\binom{n}{2}$.